
ROBUST MULTI-OBJECTIVE CONTROLLED DECODING OF LARGE LANGUAGE MODELS

A PREPRINT

Seongho Son*
University College London
London, United Kingdom
seong.son.22@ucl.ac.uk

William Bankes*
University College London
London, United Kingdom
william.bankes.21@ucl.ac.uk

Sangwoong Yoon*
University College London
London, United Kingdom
sangwoong.yoon@ucl.ac.uk

Shyam Sundhar Ramesh*
University College London
London, United Kingdom
shyam.ramesh.22@ucl.ac.uk

Xiaohang Tang
University College London
London, United Kingdom
xiaohang.tang.20@ucl.ac.uk

Ilija Bogunovic
University College London
London, United Kingdom
i.bogunovic@ucl.ac.uk

March 13, 2025

ABSTRACT

Test-time alignment of Large Language Models (LLMs) to human preferences offers a flexible way to generate responses aligned to diverse objectives without extensive retraining of LLMs. Existing methods achieve alignment to multiple objectives simultaneously (e.g., instruction-following, helpfulness, conciseness) by optimizing their corresponding reward functions. However, they often rely on predefined weights or optimize for averages, sacrificing one objective for another and leading to unbalanced outcomes. To address this, we introduce Robust Multi-Objective Decoding (RMOD), a novel inference-time algorithm that optimizes for improving worst-case rewards. RMOD formalizes the robust decoding problem as a maximin two-player game between reward weights and the sampling policy, solving for the Nash equilibrium. We show that the game reduces to a convex optimization problem to find the worst-case weights, while the best response policy can be computed analytically. We also introduce a practical RMOD variant designed for efficient decoding with contemporary LLMs, incurring minimal computational overhead compared to non-robust Multi-Objective Decoding (MOD) methods. Our experimental results showcase the effectiveness of RMOD in generating responses equitably aligned with diverse objectives, outperforming baselines up to 20%.

1 Introduction

Large Language Models (LLMs) require alignment to become useful and safe conversational agents [Rafailov et al., 2023, Azar et al., 2023, Hong et al., 2024, Ethayarajh et al., 2024, Wu et al., 2024]. However, human preferences are diverse and nuanced, leading recent work to frame alignment as a multi-objective problem [Zhao et al., 2023, Shi et al., 2024] over a variety of desirable attributes and alignment objectives, for example, *helpfulness*, *safety*, *honesty*, and *conciseness*. Test time alignment [Mudgal et al., 2023] enables flexible control over the importance of different objectives at inference time without expensive retraining. This is a useful property as the alignment of an LLM can be varied to address a specific task, prompt, or interaction with a variety of users with diverse preferences [Sorensen et al., 2024b].

Existing methods for multi-objective alignment often formalize this problem through a weight vector that characterizes the relative importance of the objectives at deployment [Shi et al., 2024, Wang et al., 2024b,a, Rame et al., 2024]. In practice, the correct weighting of objectives is often unknown, leading to models that over-optimize specific alignment goals whilst under-prioritizing others. To address this problem, recent work has proposed several solutions, including treating weights as hyperparameters [Shi et al., 2024], learning specific weightings for different groups [Zhao et al.,

*Equal Contribution.

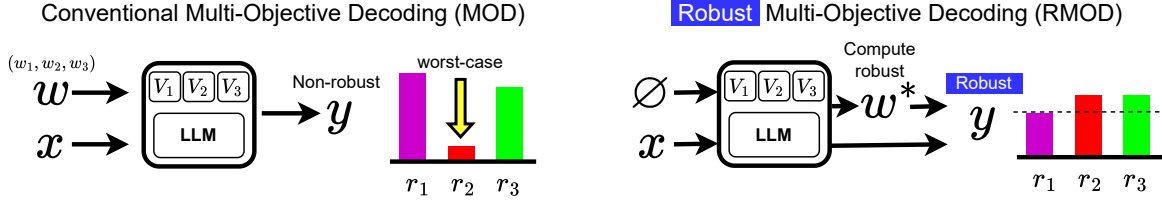


Figure 1: (Left) Existing multi-objective alignment methods require the weights for each reward. (Right) RMOD produces a robust response y when a prompt x is given, using the worst-case weights w^* computed by solving a min-max problem. RMOD effectively improves the worst-case reward without requiring externally given weights.

2023], or learning weights from previous conversation examples [Poddar et al., 2024]. These approaches rely on user information or records of previous interactions that may not be available at inference time. Furthermore, a single set of weights may not be suitable in specific applications as weights on different objectives may depend on the prompt or even vary over time within a conversation with the LLM [Carroll et al., 2024].

In this work, we introduce **Robust Multi-Objective Decoding (RMOD)**, a novel robust test-time alignment algorithm designed to tackle the challenge of improving worst-case rewards across diverse objectives. Unlike existing approaches, RMOD dynamically reweights alignment objectives to improve the least aligned objective; see Figure 1. Our main contributions are:

- (i) We propose an algorithm that achieves balanced alignment without requiring any information about the relative importance of the objectives;
- (ii) We present a practical variant of RMOD that performs blockwise best-of- K w.r.t. the worst-case weighted sum of values, incurring minimal compute overhead;
- (iii) We rigorously evaluate RMOD on diverse multi-objective datasets, demonstrating the effectiveness of our method in robust alignment. Our results demonstrate that RMOD achieves a win rate of over 57% and 70% in the UltraFeedback [Cui et al., 2023] dataset and Helpful-Harmless [Bai et al., 2022a] datasets, respectively, against the reference policy, while consistently outperforming other baselines. In summary:

RMOD provides a low-latency, inference-time alignment that significantly improves the balance between alignment objectives without any information about the objective weights.

1.1 Related Work

Multi-objective alignment of policies [Li et al., 2020] is an important area of research in reinforcement learning, particularly in contexts where agents must balance competing objectives. In the case of LLMs, recent work has argued that optimizing for multiple objectives is essential to correctly align LLMs [Vamplew et al., 2018], as modern applications demand a range of alignment goals [Wang et al., 2024a], including helpfulness, safety, and instruction-following, among others. Aligning to diverse objectives is key to personalized [Wang et al., 2023, Chen et al., 2024] and pluralistic alignment [Sorensen et al., 2024b, Kirk et al., 2024] approaches, which aim to align LLMs to a diverse range of cultures and world views.

A common approach to aligning models with multiple objectives is to weight different alignment objectives at training [Zhou et al., 2023, Dong et al., 2023] or inference time [Shi et al., 2024, Wang et al., 2024b, Dong et al., 2023, Rame et al., 2024]. The weights on these objectives can be provided as a context [Shi et al., 2024, Wang et al., 2024b, Dong et al., 2023] to the model; used to combine the weights of a diverse set of models [Rame et al., 2024, Feng et al., 2024, Jang et al., 2023]; or are included within the prompt itself [Wang et al., 2024a, Castricato et al., 2024]. These weights are a key component in ensuring the correct model alignment but are often not known in practice. Carroll et al. [2024] argue that the weighting of different alignment objectives can even change during interactions.

To address this, Shi et al. [2024] propose finding weightings using a hyperparameter search across a validation set - this one-size-fits-all approach lacks the flexibility to distribution shifts away from the validation set at inference time. Mavromatis et al. [2024] merge models to minimize the perplexity of the input prompt, and Zhao et al. [2023] propose to implicitly weight objectives using learnt contexts for different groups at inference time, however, one must be careful in how these groups are selected. Hwang et al. [2023], Li et al. [2023] show that demographic information is not necessarily predictive of the correct alignment of individuals. Finally, Poddar et al. [2024], Chen et al. [2024] leverage previous interactions to learn a model that predicts suitable weights across attributes. All these directions

require additional information at inference time, be it about the users themselves or examples of prior interactions. This information is not always available or can be misleading. Thus, we propose that a robust multi-objective alignment approach is desirable in practice such that LLMs are equitably aligned to a variety of attributes.

Although other works Ramesh et al. [2024], Chakraborty et al. [2024], Maura-Rivero et al. [2025] have considered robust alignment over a group of attributes, we are the first to consider such an objective in the inference time alignment setting. Inference time approaches, such as those introduced in Mudgal et al. [2023], Zhou et al. [2024], Kong et al. [2024], Khanov et al. [2024] offer more flexibility than fine-tuning methods, as their alignment can be easily changed without further retraining. Test-time approaches also offer further performance improvements through scaling test time compute Snell et al. [2024].

2 Problem Formulation

Let $\pi_{\text{ref}}(\cdot)$ denote a reference language model that generates a response y for a given prompt $x \in \mathcal{X}$, where \mathcal{X} is the set of prompts. The response $y = [y_1, \dots, y_T]$ consists of T tokens where each token y_t is drawn from the token vocabulary \mathcal{Z} . We denote the probability of response y given the prompt x as $\pi_{\text{ref}}(y|x)$. We aim to adapt responses y sampled from $\pi_{\text{ref}}(\cdot|x)$ to align with *multiple objectives at inference time*. Specifically, we define our objectives through reward models that evaluate the desirability of a response w.r.t. various attributes (e.g., conciseness, harmlessness, accuracy, etc.). We denote the objectives as $g \in \mathcal{G}$, where $|\mathcal{G}| = G$. We denote the reward models as $\mathcal{R}_G = \{R_g(x, y)\}_{g=1}^G$ corresponding to G objectives. Here, $R_g(x, y)$ is a scalar function embodying objective g that evaluates how desirable the response y given the prompt x is. Following standard practices in the literature [Dai et al., 2023, Ouyang et al., 2022, Mudgal et al., 2023], we define a token-wise reward R_g as

$$R_g(x, y^t) = \begin{cases} 0 & \text{if } y_t \neq \text{EOS}, \\ r_g(x, y^t) & \text{if } y_t = \text{EOS}. \end{cases} \quad (1)$$

Here, $y^t = [y_1, \dots, y_t]$ denotes a subsequence of t tokens, where each token y_t is drawn from the token vocabulary \mathcal{Z} . Moreover, we use the reward function $r_g(\cdot, \cdot)$ to evaluate the reward of the final response y . The alignment of response y to the G objectives is measured through the weighted multi-objective reward $\sum_{g=1}^G w_g R_g(x, y)$. Here, $w = (w_1, \dots, w_G)$, and Δ^{G-1} represent weights over the $(G - 1)$ -dimensional simplex and express the significance over the reward objectives. However, in real-world scenarios, the relative significance w among the G objectives is often *unknown*. User preferences vary widely based on context, culture, geography, etc., e.g., prioritizing helpfulness over harmlessness [Bai et al., 2022b], preferring conciseness over detailed, truthful responses [Cui et al., 2023], or emphasizing values like justice and duty over compassion and respect [Sorensen et al., 2024a]. Unlike prior works such as Shi et al. [2024], which assume *exact* user preferences are predefined at test time in terms of weight vectors, we consider the scenario where this assumption fails due to any number of reasons; for example, (i) **First-time users**: It is challenging to determine their preferences due to a lack of prior interactions [Kang et al., 2023], (ii) **Noisy or misspecified preference history**: Shared accounts can create conflicting interaction histories, leading to inaccurate user preferences [Jiang et al., 2018, Ma et al., 2019], (iii) **Evolving preferences**: User preferences can change over time due to new experiences [Son et al., 2024, Carroll et al., 2024].

This raises a key question: *i) Given a prompt at inference time, how can we determine the appropriate weightings over the objectives to align our response?* Moreover, efficiently decoding the response is crucial to avoid user dissatisfaction caused by high latency at inference time. For example, Best-of-K rejection sampling Stiennon et al. [2020], Nakano et al. [2021], Touvron et al. [2023] samples K i.i.d. complete responses from the reference model and chooses the response with the highest reward leading to high latency. This raises the second crucial question: *ii) How can we efficiently generate an aligned response with low latency?*

In order to tackle the aforementioned issues, we propose to generate “robust responses”, *maximizing alignment to the worst-case weightings over the objectives*, thereby ensuring equitable rewards across the objectives. Moreover, we consider a *block-wise generation* procedure (as in Mudgal et al. [2023]) in order to efficiently generate the response y . In essence, at each decoding step t given prompt x and partially decoded response y^t , we seek a robust policy $\pi^*(\cdot|x, y^t)$, that is aligned to the worst-case weightings over the G objectives and provides probabilities over vocabulary \mathcal{Z} for the next sequence z . We formalize this objective in Section 2.2.

2.1 Value Function

We formalize the robust objective for policy $\pi(\cdot|x, y^t)$ at each decoding step t using *value* functions V_g for $g \in \mathcal{G}$. This is crucial to accurately measure the alignment of the expected response towards the G objectives at each step t . Given the policy π_{ref} and the reward $R_g(\cdot)$ corresponding to group g , the value of a partial sequence y^t is the expected reward

attained by following policy π_{ref} and expressed as:

$$V_g(x, y^t) := \mathbb{E}_{z_1, z_2, \dots \sim \pi_{\text{ref}}} \left\{ \sum_{\tau \geq 1} R_g(x, [y^{t+\tau-1}, z_\tau]) \right\}, \quad (2)$$

where, $z_\tau \sim \pi_{\text{ref}}(\cdot | x, y^{t+\tau-1})$ and $y^{t+\tau} = [y^{t+\tau-1}, z_\tau]$. We denote the value of choosing a particular sequence z at the next step $t+1$ and following the reference policy π_{ref} afterward as $V_g(x, y^t; z)$. Moreover, we define the value function of a given policy π as the expected value after sampling z at the next step $t+1$ from π :

$$V_g(x, y^t; \pi) = \mathbb{E}_{z \sim \pi} [V_g(x, y^t; z)]. \quad (3)$$

2.2 Robust Objective

We describe the objective for a robust policy as a *max-min game* at each decoding step t in terms of $V_g(x, y^t; \pi)$,

$$\max_{\pi} \min_{w \in \Delta^{G-1}} \lambda \sum_{g=1}^G w_g V_g(x, y^t; \pi) - D_{\text{KL}}(\pi \parallel \pi_{\text{ref}}). \quad (4)$$

Here, the value function V_g quantifies the impact of selecting a specific sequence z at decoding step t on the expected reward $R_g(x, y^T)$ of the fully decoded response y^T . We regularize this objective with the KL divergence to ensure that the response remains probable under the reference policy π_{ref} w.r.t. a trade-off parameter λ . Moreover, the above optimization problem is a two-player zero-sum game, where the policy π and weights w act as opponents with inversely related payoffs. The policy π and the weights w represent stochastic (mixed) strategies, modeled as categorical distributions of choosing sequence z and group g , respectively.

3 Robust Multi-Objective Decoding

In this section, we discuss our proposed algorithm for solving the robust objective outlined in Equation (4). We also discuss an alternative approach to solving max-min game in Appendix D, which is no-regret learning. We begin by discussing the properties of this maxmin problem defined by this objective.

The objective in Equation (4) is clearly linear in w . Moreover, it is concave in π because the value function $V_g(x, y^t; \pi)$ is linear in π , and the KL-divergence $D_{\text{KL}}(\pi \parallel \pi_{\text{ref}})$ is convex in π . We assume that the space of $\pi(\cdot | x, y^t)$ is a convex class of probability measures. Hence, as the set of strategies for both players (π and w) are compact and correspond to mixed strategies, the existence of a Nash Equilibrium (NE) for Equation (4) is guaranteed due to Nash's existence theorem [Nash Jr, 1950].

3.1 Minimax Reformulation

The objective in Equation (4) is concave-convex in terms of π and w and allows the interchange of minimum and maximum operators due to the minimax theorem [v. Neumann, 1928, Sion, 1958]. Thus, for each decoding step t we can re-write Equation (4) as

$$\min_{w \in \Delta^{G-1}} \max_{\pi} \lambda \sum_{g=1}^G w_g V_g(x, y^t; \pi) - D_{\text{KL}}(\pi \parallel \pi_{\text{ref}}). \quad (5)$$

Note that the inner maximization in Equation (5) is in line with the standard KL-regularized RLHF objective. Here, $\lambda > 0$ trades off the weighted value of policy π for a deviation of π from the reference model π_{ref} . Moreover, due to the strict convexity of $D_{\text{KL}}(\pi \parallel \pi_{\text{ref}})$ w.r.t. π for a fixed π_{ref} , the maximization problem is strictly concave. Consequently, the optimal policy for the inner maximization problem is unique for any given weights w and trade-off parameter λ , and we characterize the policy in the following proposition.

Proposition 3.1. *Given the value functions V_g for each objective $g \in \mathcal{G}$, the solution to the inner maximization problem in Equation (5) is unique for any given weights w and trade-off parameter λ , and can be expressed as*

$$\pi(z | [x, y^t]; w) = \frac{\pi_{\text{ref}}(z | [x, y^t]) \exp \left(\lambda \sum_{g=1}^G w_g V_g(x, y^t; z) \right)}{Z(x, y^t, w)}, \quad (6)$$

where, $Z(x, y^t, w)$ is a normalization constant.

Algorithm 1 Robust Multi-Objective Decoding (RMOD)

```

1: Input: Prompt  $x$ , group value functions  $V_g$  for  $g \in \mathcal{G}$ , reference policy  $\pi_{\text{ref}}$ , action space  $\mathcal{Z}$ 
2: // Solve a NE at each decoding step  $t$ 
3: for  $t \in [T]$  do
4:   Calculate  $V_g(x, y^t; z)$  for all  $g \in \mathcal{G}$ ,  $z \in \mathcal{Z}$ 
5:   // Weights solving
6:   Obtain  $w^*$  by solving Equation (7)
7:   // Policy solving via Best Response
8:   Obtain  $\pi^*(\cdot | [x, y^t]) = \pi(\cdot | [x, y^t]; w^*)$  by substituting  $w = w^*$  in Equation (6)
9:   // Sample next sequence and concatenate
10:  Sample  $z \sim \pi^*(\cdot | [x, y^t])$ 
11:   $y^{t+1} = [y^t; z]$ 
12: end for
13: Return  $y^T$ 

```

Here, the weights-conditioned policy, $\pi(\cdot | \cdot; w)$, is the *best-response policy* to weights w . We defer the proof of this proposition to Appendix A.1.

Proposition 3.1 establishes that given a set of weights w , the reference policy π_{ref} , and the value functions V_g , one can employ Equation (6) to sample from a policy that aligns with the objectives while staying close to the reference policy in terms of KL divergence. Moreover, it enables us to develop an inference-time alignment method that keeps the reference model frozen while combining its logits with the value functions V_g to achieve the alignment objective.

Plugging Equation (6) back to Equation (5), we obtain the following simplified optimization problem with respect to w (derivation is provided in Appendix A.3):

$$\begin{aligned}
 w^* &= \arg \min_{w \in \Delta^{G-1}} \log \mathbb{E}_{z \sim \pi_{\text{ref}}(\cdot | [x, y^t])} [f(z; x, y^t, w)], \\
 \text{and } f(z; x, y^t, w) &= \exp \left(\sum_{g=1}^G \lambda w_g V_g(x, y^t; z) \right).
 \end{aligned} \tag{7}$$

Here, w^* is the Nash equilibrium solution of Equation (4). And we obtain the corresponding *best-response policy*, $\pi^* = \pi(\cdot | \cdot; w^*)$ by substituting w^* in Equation (6). We formally detail this in the following proposition.

Proposition 3.2. *The solution w^* to the convex optimization problem in Equation (7) and $\pi^* = \pi(\cdot | \cdot; w^*)$ in Equation (6) constitute a Nash Equilibrium for the max-min game in Equation (4).*

In contrast to the initial objective presented in Equation (4), Equation (7) represents a non-linear optimization problem solely in terms of the variable w . Notably, Equation (7) constitutes a convex optimization problem, owing to the inclusion of the *LogSumExp* function, which is known to be convex [El Ghaoui, 2017]. This convexity guarantees the existence of a global minimum, which can be identified through the search for a local minimum. Furthermore, the dimensionality of w is generally smaller than that of the space defined by π , making Equation (7) amenable to solve by using iterative techniques such as gradient descent, which can efficiently approximate the optimal solution.

We note that the evaluation of $\pi_{\text{ref}}(z | [x, y^t])$ and $V_g(x, y^t; z)$ is performed only once as $\pi_{\text{ref}}(z | [x, y^t])$ and $V_g(x, y^t; z)$ are independent of w . Hence, in order to solve Equation (7), we propose to run an iterative algorithm based on the inferred values V_g to find the worst-case weights w^* that minimizes the exponential of the weighted values.

3.2 RMOD Algorithm

Finally, we detail the theoretical version of our method in Algorithm 1 that outputs a robust response y^T of length T for a given prompt x . At each decoding step t , it is necessary to solve for a Nash Equilibrium of Equation (4) in order to determine the robust decoding policy for sampling the next token sequence z . We first obtain w^* (min-player) by solving the simplified problem in Equation (7). This requires the evaluation of the value functions V_g . Then we derive the max-player $\pi^* = \pi(\cdot | \cdot; w^*)$ by computing the best response to w^* , i.e. substituting w^* into Equation (6). Finally, we sample z from $\pi^*(\cdot | [x, y^t])$, concatenate it to the previously decoded subsequence, and enter the next decoding step.

The RMOD algorithm is theoretically designed to yield a robust policy at each decoding step. However, in practical applications, minimizing the latency of RMOD remains a critical objective. In Algorithm 1, the computation of weights in Line 6, which requires a summation over all possible values of z , and the computation of the Best Response policy

Algorithm 2 Practical Version of RMOD

```

1: Input: Prompt  $x$ , learnt group value functions  $V_g(\cdot; \theta)$  for  $g \in \mathcal{G}$ , reference policy  $\pi_{\text{ref}}$ , action space  $\mathcal{Z}$ , the
   regularisation coefficient  $\lambda > 0$ , candidate number  $K$ , block size  $B$ , weight update iteration limit  $I$ 
2:  $y^0 = \emptyset$ 
3: for  $t \in [T]$  do
4:   // Sample  $K$  blocks of length  $B$ 
5:    $z_{(k)} \sim \pi_{\text{ref}}(\cdot | [x, y^t]) \forall k \in [K]$ 
6:   // Calculate values of blocks
7:    $V_g(x, y^t; z_{(k)}, \theta)$  for all  $g \in \mathcal{G}$ ,  $k \in [K]$ 
8:   // Iteratively solve for weights
9:   Update weights (Equation (12))  $I$  times:  $w_{g,i+1} = w_{g,i} \cdot \exp \left[ -\eta \sum_{k=1}^K \pi_{\text{ref}}(z_k | [x, y^t]) h(z_k; x, y^t, w_i, g) \right]$ 
10:  // Choose block
11:   $y_{t+1} = \arg \max_{z_{(k)}} \sum_{g=1}^G w_{g,I} \cdot V_g(x, y^t; z_{(k)}, \theta)$ 
12:  // Append the selected block
13:   $y^{t+1} = [y^t, y_{t+1}]$ 
14: end for
15: Return  $y^T$ 

```

in Line 8 both significantly contribute to the latency challenges inherent to RMOD. In Section 4, we introduce practical components designed to mitigate the high-latency challenges associated with the RMOD algorithm.

3.3 The Behavior of Optimal Weights in RMOD

We analyze Equation (7) using the KKT conditions in Appendix B to study the behaviour of w^* . We show that the weights w_g^* equalize the expected future rewards across groups, leading to robust alignment over multiple objectives. The value of λ determines the sparsity of w^* . Low values of λ result in high entropy across the weights whilst high values of λ lead to a low entropy with the majority of weight applied to a single group.

4 Practical Implementation of RMOD

In this section, we introduce a practical, low-latency implementation of Robust Multi-Objective Decoding (RMOD) outlined in Algorithm 2. In particular, we discuss the training of the value functions V_g using the reward models R_g , and introduce two key approximations to improve the efficiency of our RMOD method: (i) Approximate evaluation of expectation over $z \sim \pi_{\text{ref}}$ in Equation (7) to obtain w^* , and (ii) Approximate sampling of z from *Best Response* policy in Equation (6), where $w = w^*$. Additionally, we employ gradient descent on weights w to solve Equation (7). Next, we discuss each of these techniques in detail.

4.1 Training the Value Functions

Note that Algorithm 1 requires the evaluations from group value functions V_g , whereas we are only given the reward models corresponding to the G objectives. Therefore, our goal is to train G value functions that approximate $V_g(\cdot, \cdot)$ for each $g \in \mathcal{G}$.

The parameters θ of the value function V_g are then trained over a set of training prompts μ to minimize the following loss:

$$\mathbb{E}_{x \sim \mu, y \sim \pi_{\text{ref}}(\cdot | x)} \sum_{1 \leq t \leq |y|} (V_g(x, y^t; \theta) - V_g(x, y^t))^2. \quad (8)$$

However, since the values from the true V_g are unavailable, we follow the **CD-FUDGE** [Yang and Klein, 2021] approach to train the value functions using the rewards of the final response $r_g(x, y)$:

$$\mathbb{E}_{x \sim \mu, y \sim \pi_{\text{ref}}(\cdot | x)} \sum_{1 \leq t \leq |y|} (V_g(x, y^t; \theta) - r_g(x, y))^2. \quad (9)$$

We discuss further details regarding the training of value functions for the experiments in Section 5.

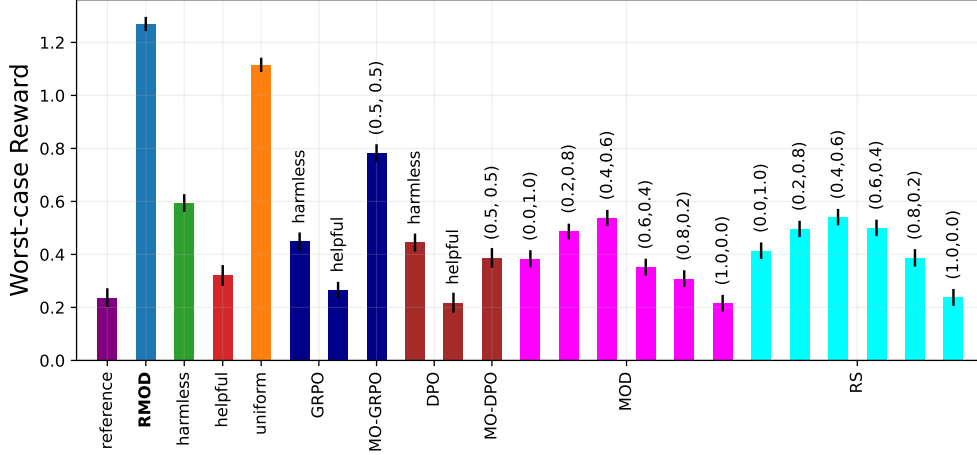


Figure 2: Worst-case reward obtained by RMOD and baselines in the **HH** dataset. We use $B = 16$ for all the decoding methods and $\lambda = 0.5$ for RMOD. Texts at the top of bars indicate the reward or weighted sum of rewards used for the corresponding method. RS and MOD use the models trained with GRPO. RMOD shows significantly higher worst-case reward than all the baselines, regardless of whether they are fine-tuned or aligned at inference time.

4.2 Approximate Computation of Optimal Weights

Our proposed value function architecture from Section 4.1 predicts the values of $V_g(x, y^t; z)$ for each z individually. Consequently, one needs to perform $|\mathcal{Z}|$ forward passes through the trained value function to evaluate the expectation over all possible sequences $z \in \mathcal{Z}$ in Equation (7). We note that in practical settings $|\mathcal{Z}|$ is large and when $|z| > 1$, i.e., a block of tokens or sentence (see Section 4.4), $|\mathcal{Z}|$ can grow exponentially.

We thus turn to approximate the expectation in the objective function in Equation (7) with a set of independent samples $\{z_k\}_{k=1}^K$, where $z_k \sim \pi_{\text{ref}}(\cdot | [x, y^t])$, $k = 1, \dots, K$ (see Line-4 of Algorithm 2). Then, we approximate the optimal weight w^* with \hat{w}^* as follows:

$$\hat{w}^* = \arg \min_{w \in \Delta^{G-1}} \log \sum_{k=1}^K \pi_{\text{ref}}(z_k | [x, y^t]) f(z_k; x, y^t, w). \quad (10)$$

Thus, instead of solving the exact objective (see Equation (7)) as done in Line-6 of Algorithm 1, we propose to solve the approximated objective in Equation (10) and use \hat{w}^* . As discussed before in Proposition 3.2, Equation (10) is a convex optimization problem and hence guaranteed to have a global minimizer. However, it is not possible to obtain a closed-form solution for Equation (10) directly. Hence, we propose to use iterative methods such as projected gradient descent (GD) to attain the global minimizer. We note that due to the monotonically increasing nature of log function, the minimizer of Equation (10) is the same as the minimizer of

$$\hat{w}^* = \arg \min_{w \in \Delta^{G-1}} \sum_{k=1}^K \pi_{\text{ref}}(z_k | [x, y^t]) f(z_k; x, y^t, w). \quad (11)$$

Further, we adopt a soft update by performing gradient descent w.r.t. the logits of the group weights, i.e., $\log w$. The corresponding update expression for w is

$$w_{g,i+1} := w_{g,i} \cdot e^{-\eta \sum_{k=1}^K \pi_{\text{ref}}(z_k | [x, y^t]) h(z_k; x, y^t, w_{g,i})} \quad (12)$$

for $h(z; x, y^t, w, g) = e^{\sum_{g=1}^G \lambda w_g V_g(x, y^t; z)} \lambda w_g V_g(x, y^t; z)$. We defer the derivation of this update to Appendix A.4.

Hence, at each decoding step t , given K independent samples $\{z_k\}_{k=1}^K$ from $\pi_{\text{ref}}(\cdot | [x, y^t])$, we initialize the weights as $w_0 = \{1/G, \dots, 1/G\}$, and iteratively update it using Equation (12) (see Line-9 of Algorithm 2). This effectively approximates the solving of Equation (7) in Line-6 of Algorithm 1 for practical settings.

4.3 Direct Sampling from Best Response Policy

Following I iterations of weight updates as outlined in Line-9 of Algorithm 2, we obtain the robust policy by substituting the converged weights, $w = w_I$, back to Equation (6). However, exact computation of the best response

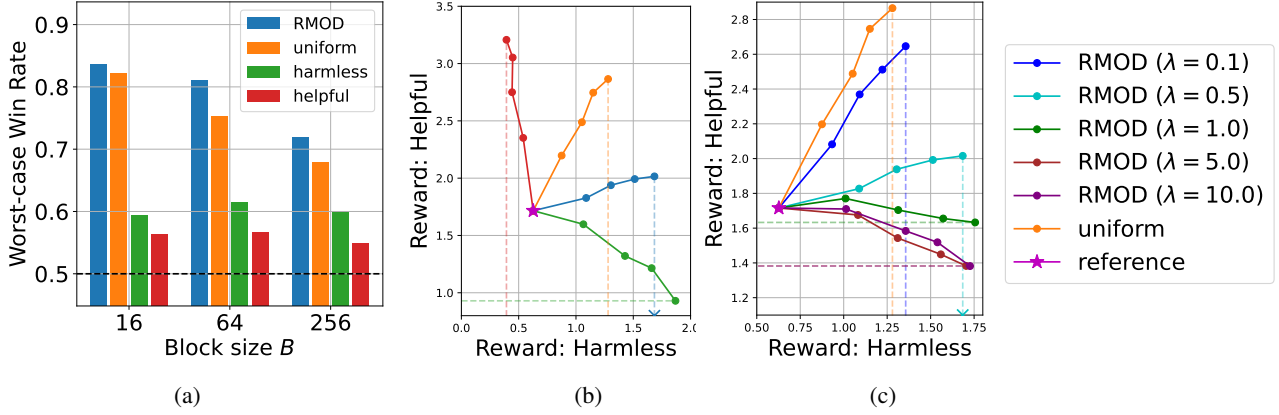


Figure 3: (3a-3b) Comparative study on the **HH dataset** between different decoding methods. We use $\lambda = 0.5$ for RMOD. In Figure 3a, we present the worst-case win rates against the reference policy across block sizes $B \in \{16, 64, 256\}$. As B decreases from 256 to 16, the worst-case win rate of RMOD increases, consistently outperforming the baselines. Figure 3b show the rewards obtained with $B = 16$ for different values of K , while sharing the same legend as Figure 3a. The purple star represents the average reward of π_{ref} , and the dots represent increasing K values (2, 4, 8, 16) as they move away from the purple star. RMOD improves the worst-case reward, having higher harmlessness reward than UNIFORM. (3c) Testing different values of λ for RMOD in the **HH dataset**. We ablate the performance of RMOD against the value of λ with $B = 16$ and demonstrate that smaller values of λ reduces RMOD to UNIFORM decoding. On the other hand, as λ increases, RMOD concentrates on improving the worst-case reward.

policy $\pi(\cdot|[x, y^t]; w_I)$ is still expensive as one needs to calculate $\pi(z|[x, y^t]; w_I)$ for each z individually, wherein the cardinality of $z \in |\mathcal{Z}|$ can be large. To mitigate this, we reuse the existing samples $\{z_k\}_{k=1}^K$ for efficiency and choose sample z_k with the highest weighted average value, $\sum_{g=1}^G \lambda w_{g,I} V_g(x, y^t; z_k)$ (see Line-11 of Algorithm 2). This avoids additional evaluations using the reference model or the value function and reduces computational costs.

4.4 Block-wise RMOD

The length of the sequence z plays a crucial role in the computation cost and alignment performance of the decoding algorithm. The number of decoding steps T , executed by Algorithm 2 for a given prompt x , reduces as the length of z increases. When z corresponds to a single token, the decoding process simplifies to token-wise decoding. However, this method requires computing the values for all samples, $\{z_k\}_{k=1}^K$, at each token, resulting in high computational costs (see Line-7 of Algorithm 2). To address this limitation, we adapt the RMOD algorithm to incorporate blockwise decoding [Mudgal et al., 2023], as detailed in Algorithm 2. In this formulation, z represents a block of B tokens, where B can range from one to the maximum token length for each response. Notably, when each block constitutes a complete response, blockwise RMOD corresponds to a robust version of Best-of- K rejection sampling [Stiennon et al., 2020, Nakano et al., 2021, Touvron et al., 2023], wherein the response with the maximum weighted-average value is selected. In Algorithm 2, at each step t , an entire block of B tokens is selected from K generated candidates. This modification significantly reduces the required number of value function evaluations compared to token-wise decoding, thereby enhancing the scalability of our algorithm.

5 Experiments

In this section, we study the empirical performance of RMOD on various multi-objective datasets. Our code² is available online, and further details on the experimental setup and results can be found in Appendix C.

5.1 Experiment Settings

Datasets. We evaluate RMOD on the Anthropic Helpfulness-Harmless (HH) [Bai et al., 2022a], UltraFeedback [Cui et al., 2023] and ValuePrism [Sorensen et al., 2024a] datasets. We construct our training set for value function learning by generating 4 responses per prompt from π_{ref} on the training split of all datasets.

²Code available at: <https://github.com/williambankes/robust-multi-objective-decoding>.

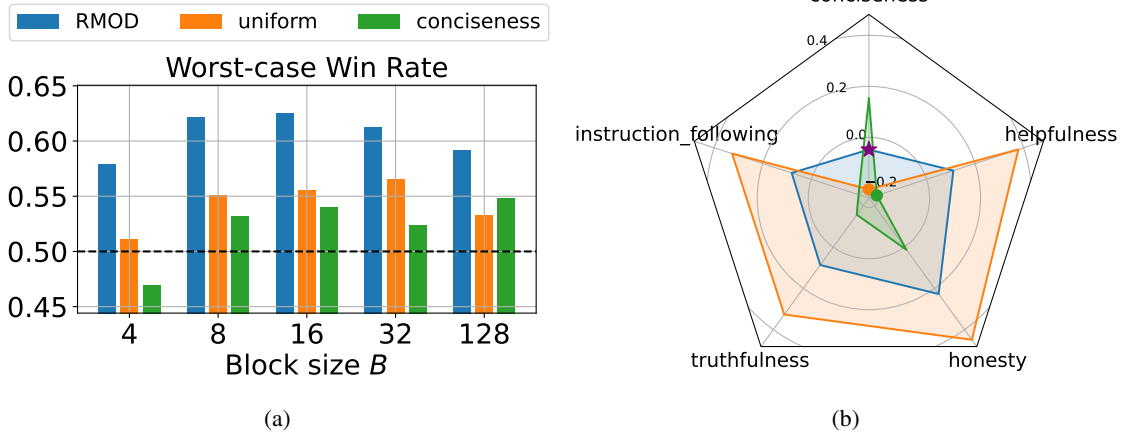


Figure 4: Performance comparison of decoding algorithms on **UltraFeedback** (Figure 4a- 4b). Figure 4a displays worst-case win rates in the UltraFeedback dataset for block sizes $B \in \{4, 8, 16, 32, 128\}$ and $K = 16$. RMOD achieves higher than 57% win rate against the reference policy and consistently outperforms UNIFORM decoding. Figure 4b displays average reward in the UltraFeedback dataset with $B = 4$. The purple star denotes the worst-case reward of RMOD and corresponds to the conciseness objective, and is much higher than that of UNIFORM decoding and CONCISENESS (orange, green dots).

Language Models. We use `gemma-2-2b-it` as the reference model for all experiments. For each dataset, we use pre-existing reward models to evaluate the generated responses. For the HH dataset, we use `gpt2-large-harmless-reward_model` and `gpt2-large-helpful-reward_model` to generate harmless and helpful rewards respectively. For the UltraFeedback dataset, we use the relevant reward heads from ArmoRM [Wang et al., 2024a]. Finally, for the ValuePrism dataset we use `tsor13/kaleido-x1` to generate rewards for different values, including 'Autonomy', 'Right to life', 'Justice' and 'Compassion'. Further details can be found in Appendix C.

Algorithms. We train the value functions (see Section 4.1) using an MSE-loss w.r.t. the rewards of the responses in the training set, as per CD-FUDGE [Yang and Klein, 2021, Mudgal et al., 2023]. As baselines, we compare RMOD against other non-robust controlled decoding strategies that either align with individual reward objectives or optimize for the uniformly weighted rewards across all objectives (UNIFORM), i.e., $w_g = \frac{1}{|G|}$. In the HH dataset, We also present Group Relative Preference Optimization [Shao et al., 2024, GRPO], Direct Preference Optimization [Rafailov et al., 2023, DPO], Rewarded Soup [Rame et al., 2024, RS], and Multi-Objective Decoding [Shi et al., 2024, MOD] baselines, which combine individual models trained with GRPO. For RS and MOD, we use (harmlessness, helpfulness) weightings of (1.0, 0.0), (0.8, 0.2), (0.6, 0.4), (0.4, 0.6), (0.2, 0.8), (0.0, 1.0). For GRPO and DPO, we use each of harmlessness and helpfulness reward only to train the policy. MO-GRPO uses 0.5 weight for each reward, while MO-DPO does the same to determine the preferences between the responses. See Appendix C for further implementation details.

Evaluation Metrics. To evaluate the performance of our algorithm, we compute *rewards* and *Worst-Case Win Rate*. For each dataset, we generate a set of responses from a set of held-out test prompts and evaluate them using the reward models corresponding to different alignment objectives. To calculate the worst-case win rate, we compare the minimum reward for each generated response to that of the response from the reference model, π_{ref} . If the minimum reward is greater than that of the reference model, we assign the prompt a win, $\mathbb{I}[\min_g r_g(x, y_1^T) > \min_g r_g(x, y_2^T)]$ where y_1^T and y_2^T are responses from different algorithms, respectively. We report the average win rate across 1024 test prompts for the HH dataset, 956 prompts for the UltraFeedback dataset, and 1000 prompts for the ValuePrism dataset.

5.2 Experiment Results

Does RMOD Robustly Align to Multiple Objectives?

We compute the worst-case rewards obtained by RMOD and the baselines in the HH dataset and compare them in Figure 2. RMOD significantly outperforms all the baselines, while additional baselines including RS and MOD underperform the decoding baseline UNIFORM. We note that among the baselines, methods like MO-GRPO that combine the rewards similarly to UNIFORM decoding achieve higher worst-case rewards than other combinations. In Figure 3, we show how the responses generated by UNIFORM, a single objective, and RMOD align to the helpful and harmless objectives in the HH dataset. Both single-objective baselines sacrifice performance in the other objective to prioritize a single alignment reward, leading to poor alignment across the other objective. The baseline UNIFORM

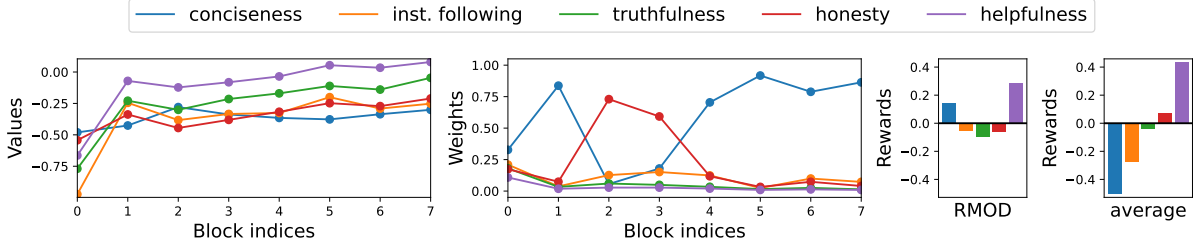


Figure 5: Analysis of RMOD’s weight and value predictions on **UltraFeedback** dataset while generating a response with $K = 16$ candidates, and block size $B = 16$ for a single prompt. RMOD adapts its weights for each block and follows the dynamic changes in worst-case value, mainly between conciseness and honesty in this case. We note that RMOD’s generated response significantly outperforms the response generated by UNIFORM decoding in terms of worst-case reward and highlights the robustness of our method.

improves both objectives; however, it improves helpfulness much more than harmlessness, also resulting in unequal alignment. RMOD specifically targets the worst performing value for each prompt, outperforming baselines up to 20% in the worst-case win rates. In our results from the Ultrafeedback dataset, shown in Figure 4b, RMOD similarly improves the worst-case reward over the five alignment objectives (conciseness in this case). When conducting a response-wise comparison w.r.t. the reference model, via the worst-case win rate, RMOD consistently outperforms UNIFORM and the single-objective CONCISENESS baseline (often the worst-performing alignment objective).

How Do λ and Block Size B Affect RMOD?

To gain further insight into the RMOD algorithm, we perform ablation experiments across block size B and tradeoff parameter λ . In Figure 3 we test $\lambda \in \{0.1, 0.5, 1.0, 5.0, 10.0\}$ on the HH dataset. As noted in Section 3.3, we expect λ to control the sparsity of the weights across different objectives. Our empirical results support this conclusion; as the value of λ increases, the sparsity of the weights also increases and concentrates on the worst reward, in this case, harmlessness. For low values of λ , the weights are non-sparse and more equal, thus leading RMOD to behave similarly to the UNIFORM decoding baseline. Hence, RMOD can be tuned to express a broad range of policies through λ .

The block size B is another key hyperparameter. On the HH dataset (Figure 3a), we observe that as the block size increases from 16, the win rate of all the decoding algorithms decreases. As shown in Mudgal et al. [2023], Beirami et al. [2024] the KL divergence between a blockwise decoding policy π and the reference policy π_{ref} (see Equation (4)) is upper bounded by a function inversely proportional to the block size. Thus, as the block size increases, RMOD stays closer to the reference policy. We repeat this experiment on the Ultrafeedback dataset as shown in Figure 4a and observe that the worst-case win rates of algorithms are higher at $B \in \{16, 32\}$, while being the lowest for the smallest block size 4. This could indicate that for blocks that are very short, it becomes harder for the value function to accurately predict the differences between the future expected rewards of sampled blocks.

How robust is RMOD as the number of different alignment objectives increases?

We investigate how the worst-case reward of RMOD varies as the number of alignment objectives increases on the ValuePrism dataset. As shown in Figure 6, we decode responses using an increasing subset of the 10 most frequent rewards in the dataset and compare the worst-case rewards of the RMOD and UNIFORM decoding. We find that RMOD outperforms the UNIFORM decoding baseline, regardless of the increase in the number of objectives considered. However, both methods show decreased performance as the number of objectives increases. We hypothesize that for larger numbers of objectives, the trade-off between diverse rewards increases the difficulty of robust alignment, as improving one objective is more likely to sacrifice performance on multiple other objectives. In Figure 6b, we reverse the order of the 10 most frequent rewards being added to the considered subset. We note that the worst-case reward is much lower at two objectives, suggesting that the performance drop in Figure 6a at 10 objectives is caused by a particularly difficult objective. To investigate the trade-off between rewards further, we examine response examples within the Ultrafeedback dataset. Figure 5 shows how the value estimations and weights of a specific response vary during decoding, and we note how RMOD trades off honesty and conciseness in the weights during decoding. By putting higher weights on conciseness and instruction following rewards, RMOD achieves a much higher worst-case reward than that of UNIFORM, while showing slightly lower rewards in truthfulness, honesty, and helpfulness.

6 Conclusion

We proposed RMOD, a novel inference-time algorithm that significantly improves the balance between the rewards without any information about the weights for the objectives. We showed that RMOD solves for the Nash Equilibrium

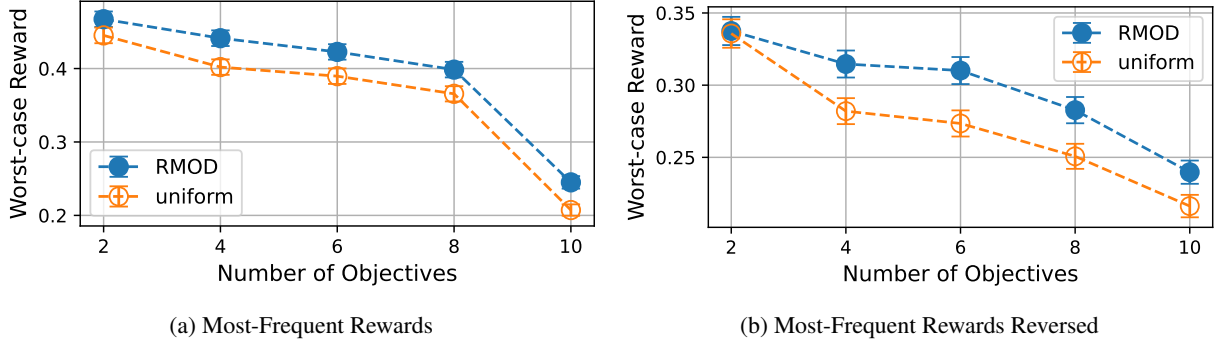


Figure 6: In Figure 6a and Figure 6b we present the worst-case rewards for RMOD and UNIFORM on the **ValuePrism** dataset [Sorensen et al., 2024a]. In Figure 6a, we observe that while the gap between the two methods remains similar, the overall rewards of both methods decrease as the number of objectives increases. In Figure 6b, we reverse the order of the objectives being added to the subset to consider and observe visibly lower worst-case reward in 2 objectives for both RMOD and UNIFORM. This shows that in Figure 6a, a particularly difficult objective was added at 10 objectives and resulted in the performance drop from the 8 objectives case.

of maximin two-player game between the policy and the objective weights, and that the game can be solved by a convex optimization. A compute-efficient variant of RMOD was proposed and compared against baselines, including UNIFORM that puts equal weights on all the objectives. When empirically tested across various multi-objective datasets, RMOD significantly improved the worst-case alignment performance in comparison to the baselines. The performance of RMOD can be affected by the biases of the reward signals and the accuracy of the trained value function, which poses additional challenges in robust alignment. We leave mitigating these issues for future work.

References

- Mohammad Gheshlaghi Azar, Mark Rowland, Bilal Piot, Daniel Guo, Daniele Calandriello, Michal Valko, and Rémi Munos. A general theoretical paradigm to understand learning from human preferences. *arXiv preprint arXiv:2310.12036*, 2023.
- Anirudhan Badrinath, Prabhat Agarwal, and Jiajing Xu. Hybrid preference optimization: Augmenting direct preference optimization with auxiliary objectives. *arXiv preprint arXiv:2405.17956*, 2024.
- Yuntao Bai, Andy Jones, Kamal Ndousse, Amanda Askell, Anna Chen, Nova DasSarma, Dawn Drain, Stanislav Fort, Deep Ganguli, Tom Henighan, et al. Training a helpful and harmless assistant with reinforcement learning from human feedback. *arXiv preprint arXiv:2204.05862*, 2022a.
- Yuntao Bai, Saurav Kadavath, Sandipan Kundu, Amanda Askell, Jackson Kernion, Andy Jones, Anna Chen, Anna Goldie, Azalia Mirhoseini, Cameron McKinnon, et al. Constitutional ai: Harmlessness from ai feedback. *arXiv preprint arXiv:2212.08073*, 2022b.
- James P Bailey and Georgios Piliouras. Multiplicative weights update in zero-sum games. In *Proceedings of the 2018 ACM Conference on Economics and Computation*, pages 321–338, 2018.
- Toygun Basaklar, Suat Gumussoy, and Umit Y Ogras. Pd-morl: Preference-driven multi-objective reinforcement learning algorithm. *arXiv preprint arXiv:2208.07914*, 2022.
- Ahmad Beirami, Alekh Agarwal, Jonathan Berant, Alexander D’Amour, Jacob Eisenstein, Chirag Nagpal, and Ananda Theertha Suresh. Theoretical guarantees on the best-of-n alignment policy. *arXiv preprint arXiv:2401.01879*, 2024.
- Micah Carroll, Davis Foote, Anand Siththaranjan, Stuart Russell, and Anca Dragan. Ai alignment with changing and influenceable reward functions. *arXiv preprint arXiv:2405.17713*, 2024.
- Louis Castricato, Nathan Lile, Rafael Rafailov, Jan-Philipp Fränken, and Chelsea Finn. Persona: A reproducible testbed for pluralistic alignment. *arXiv preprint arXiv:2407.17387*, 2024.
- Souradip Chakraborty, Jiahao Qiu, Hui Yuan, Alec Koppel, Furong Huang, Dinesh Manocha, Amrit Singh Bedi, and Mengdi Wang. Maxmin-rlhf: Towards equitable alignment of large language models with diverse human preferences. *arXiv preprint arXiv:2402.08925*, 2024.

- Daiwei Chen, Yi Chen, Aniket Rege, and Ramya Korlakai Vinayak. Pal: Pluralistic alignment framework for learning from heterogeneous preferences. *arXiv preprint arXiv:2406.08469*, 2024.
- Chirag Chhablani, Michael Sullins, and Ian A Kash. Multiplicative weight updates for extensive form games. In *Proceedings of the 2023 International Conference on Autonomous Agents and Multiagent Systems*, pages 1071–1078, 2023.
- Ganqu Cui, Lifan Yuan, Ning Ding, Guanming Yao, Wei Zhu, Yuan Ni, Guotong Xie, Zhiyuan Liu, and Maosong Sun. Ultrafeedback: Boosting language models with high-quality feedback. *arXiv preprint arXiv:2310.01377*, 2023.
- Josef Dai, Xuehai Pan, Ruiyang Sun, Jiaming Ji, Xinbo Xu, Mickel Liu, Yizhou Wang, and Yaodong Yang. Safe rlhf: Safe reinforcement learning from human feedback. *arXiv preprint arXiv:2310.12773*, 2023.
- Yi Dong, Zhilin Wang, Makesh Narsimhan Sreedhar, Xianchao Wu, and Oleksii Kuchaiev. Steerlm: Attribute conditioned sft as an (user-steerable) alternative to rlhf. *arXiv preprint arXiv:2310.05344*, 2023.
- Laurent El Ghaoui. Optimization models and applications, 2017.
- Kawin Ethayarajh, Winnie Xu, Niklas Muennighoff, Dan Jurafsky, and Douwe Kiela. Kto: Model alignment as prospect theoretic optimization. *arXiv preprint arXiv:2402.01306*, 2024.
- Shangbin Feng, Taylor Sorensen, Yuhao Liu, Jillian Fisher, Chan Young Park, Yejin Choi, and Yulia Tsvetkov. Modular pluralism: Pluralistic alignment via multi-llm collaboration. *arXiv preprint arXiv:2406.15951*, 2024.
- Yoav Freund and Robert E Schapire. A decision-theoretic generalization of on-line learning and an application to boosting. *Journal of computer and system sciences*, 55(1):119–139, 1997.
- Tingchen Fu, Yupeng Hou, Julian McAuley, and Rui Yan. Unlocking decoding-time controllability: Gradient-free multi-objective alignment with contrastive prompts. *arXiv preprint arXiv:2408.05094*, 2024.
- Jiwoo Hong, Noah Lee, and James Thorne. Reference-free monolithic preference optimization with odds ratio. *arXiv preprint arXiv:2403.07691*, 2024.
- James Y Huang, Wenxuan Zhou, Fei Wang, Fred Morstatter, Sheng Zhang, Hoifung Poon, and Muhao Chen. Offset unlearning for large language models. *arXiv preprint arXiv:2404.11045*, 2024.
- EunJeong Hwang, Bodhisattwa Prasad Majumder, and Niket Tandon. Aligning language models to user opinions. *arXiv preprint arXiv:2305.14929*, 2023.
- Joel Jang, Seungone Kim, Bill Yuchen Lin, Yizhong Wang, Jack Hessel, Luke Zettlemoyer, Hannaneh Hajishirzi, Yejin Choi, and Prithviraj Ammanabrolu. Personalized soups: Personalized large language model alignment via post-hoc parameter merging. *arXiv preprint arXiv:2310.11564*, 2023.
- Jiaming Ji, Boyuan Chen, Hantao Lou, Donghai Hong, Borong Zhang, Xuehai Pan, Juntao Dai, and Yaodong Yang. Aligner: Achieving efficient alignment through weak-to-strong correction. *arXiv preprint arXiv:2402.02416*, 2024.
- Jyun-Yu Jiang, Cheng-Te Li, Yian Chen, and Wei Wang. Identifying users behind shared accounts in online streaming services. In *The 41st International ACM SIGIR Conference on Research & Development in Information Retrieval*, pages 65–74, 2018.
- Michael Johanson, Nolan Bard, Neil Burch, and Michael Bowling. Finding optimal abstract strategies in extensive-form games. In *Proceedings of the AAAI Conference on Artificial Intelligence*, volume 26, pages 1371–1379, 2012.
- Wang-Cheng Kang, Jianmo Ni, Nikhil Mehta, Maheswaran Sathiamoorthy, Lichan Hong, Ed Chi, and Derek Zhiyuan Cheng. Do llms understand user preferences? evaluating llms on user rating prediction. *arXiv preprint arXiv:2305.06474*, 2023.
- Maxim Khanov, Jirayu Burapachee, and Yixuan Li. Args: Alignment as reward-guided search. *arXiv preprint arXiv:2402.01694*, 2024.
- Hannah Rose Kirk, Bertie Vidgen, Paul Röttger, and Scott A Hale. The benefits, risks and bounds of personalizing the alignment of large language models to individuals. *Nature Machine Intelligence*, pages 1–10, 2024.
- Lingkai Kong, Haorui Wang, Wenhao Mu, Yuanqi Du, Yuchen Zhuang, Yifei Zhou, Yue Song, Rongzhi Zhang, Kai Wang, and Chao Zhang. Aligning large language models with representation editing: A control perspective. *arXiv preprint arXiv:2406.05954*, 2024.
- Ben Krause, Akhilesh Deepak Gotmare, Bryan McCann, Nitish Shirish Keskar, Shafiq Joty, Richard Socher, and Nazneen Fatema Rajani. Gedi: Generative discriminator guided sequence generation. *arXiv preprint arXiv:2009.06367*, 2020.
- Sachin Kumar, Biswajit Paria, and Yulia Tsvetkov. Gradient-based constrained sampling from language models. *arXiv preprint arXiv:2205.12558*, 2022.

- Marc Lanctot, Kevin Waugh, Martin Zinkevich, and Michael Bowling. Monte carlo sampling for regret minimization in extensive games. *Advances in neural information processing systems*, 22, 2009.
- Seung Hyun Lee, Yinxiao Li, Junjie Ke, Innfarn Yoo, Han Zhang, Jiahui Yu, Qifei Wang, Fei Deng, Glenn Entis, Junfeng He, et al. Parrot: Pareto-optimal multi-reward reinforcement learning framework for text-to-image generation. In *European Conference on Computer Vision*, pages 462–478. Springer, 2024.
- Junyi Li, Ninareh Mehrabi, Charith Peris, Palash Goyal, Kai-Wei Chang, Aram Galstyan, Richard Zemel, and Rahul Gupta. On the steerability of large language models toward data-driven personas. *arXiv preprint arXiv:2311.04978*, 2023.
- Kaiwen Li, Tao Zhang, and Rui Wang. Deep reinforcement learning for multiobjective optimization. *IEEE transactions on cybernetics*, 51(6):3103–3114, 2020.
- Yong Lin, Hangyu Lin, Wei Xiong, Shizhe Diao, Jianmeng Liu, Jipeng Zhang, Rui Pan, Haoxiang Wang, Wenbin Hu, Hanning Zhang, et al. Mitigating the alignment tax of rlhf. In *Proceedings of the 2024 Conference on Empirical Methods in Natural Language Processing*, pages 580–606, 2024.
- Alisa Liu, Maarten Sap, Ximing Lu, Swabha Swayamdipta, Chandra Bhagavatula, Noah A Smith, and Yejin Choi. Dexperts: Decoding-time controlled text generation with experts and anti-experts. *arXiv preprint arXiv:2105.03023*, 2021.
- Alisa Liu, Xiaochuang Han, Yizhong Wang, Yulia Tsvetkov, Yejin Choi, and Noah A Smith. Tuning language models by proxy. *arXiv preprint arXiv:2401.08565*, 2024a.
- Tianlin Liu, Shangmin Guo, Leonardo Bianco, Daniele Calandriello, Quentin Berthet, Felipe Llinares, Jessica Hoffmann, Lucas Dixon, Michal Valko, and Mathieu Blondel. Decoding-time realignment of language models. *arXiv preprint arXiv:2402.02992*, 2024b.
- Muyang Ma, Pengjie Ren, Yujie Lin, Zhumin Chen, Jun Ma, and Maarten de Rijke. π -net: A parallel information-sharing network for shared-account cross-domain sequential recommendations. In *Proceedings of the 42nd international ACM SIGIR conference on research and development in information retrieval*, pages 685–694, 2019.
- Roberto-Rafael Maura-Rivero, Chirag Nagpal, Roma Patel, and Francesco Visin. Utility-inspired reward transformations improve reinforcement learning training of language models, 2025. URL <https://arxiv.org/abs/2501.06248>.
- Costas Mavromatis, Petros Karypis, and George Karypis. Pack of llms: Model fusion at test-time via perplexity optimization. *arXiv preprint arXiv:2404.11531*, 2024.
- Stephen McAleer, Kevin Wang, John Lanier, Marc Lanctot, Pierre Baldi, Tuomas Sandholm, and Roy Fox. Anytime psro for two-player zero-sum games. *arXiv preprint arXiv:2201.07700*, 2022.
- Sidharth Mudgal, Jong Lee, Harish Ganapathy, YaGuang Li, Tao Wang, Yanping Huang, Zhifeng Chen, Heng-Tze Cheng, Michael Collins, Trevor Strohman, et al. Controlled decoding from language models. *arXiv preprint arXiv:2310.17022*, 2023.
- Reiichiro Nakano, Jacob Hilton, Suchir Balaji, Jeff Wu, Long Ouyang, Christina Kim, Christopher Hesse, Shantanu Jain, Vineet Kosaraju, William Saunders, et al. Webgpt: Browser-assisted question-answering with human feedback. *arXiv preprint arXiv:2112.09332*, 2021.
- John F Nash Jr. Equilibrium points in n-person games. *Proceedings of the national academy of sciences*, 36(1):48–49, 1950.
- Long Ouyang, Jeffrey Wu, Xu Jiang, Diogo Almeida, Carroll Wainwright, Pamela Mishkin, Chong Zhang, Sandhini Agarwal, Katarina Slama, Alex Ray, et al. Training language models to follow instructions with human feedback. *Advances in Neural Information Processing Systems*, 35:27730–27744, 2022.
- Sriyash Poddar, Yanming Wan, Hamish Ivison, Abhishek Gupta, and Natasha Jaques. Personalizing reinforcement learning from human feedback with variational preference learning. *arXiv preprint arXiv:2408.10075*, 2024.
- Lianhui Qin, Sean Welleck, Daniel Khashabi, and Yejin Choi. Cold decoding: Energy-based constrained text generation with langevin dynamics. *Advances in Neural Information Processing Systems*, 35:9538–9551, 2022.
- Rafael Rafailov, Archit Sharma, Eric Mitchell, Stefano Ermon, Christopher D Manning, and Chelsea Finn. Direct preference optimization: Your language model is secretly a reward model. *arXiv preprint arXiv:2305.18290*, 2023.
- Alexandre Rame, Guillaume Couairon, Corentin Dancette, Jean-Baptiste Gaya, Mustafa Shukor, Laure Soulier, and Matthieu Cord. Rewarded soups: towards pareto-optimal alignment by interpolating weights fine-tuned on diverse rewards. *Advances in Neural Information Processing Systems*, 36, 2024.
- Alexandre Ramé, Nino Vieillard, Léonard Hussenot, Robert Dadashi, Geoffrey Cideron, Olivier Bachem, and Johan Ferret. Warm: On the benefits of weight averaged reward models. *arXiv preprint arXiv:2401.12187*, 2024.

- Shyam Sundhar Ramesh, Yifan Hu, Iason Chaimalas, Viraj Mehta, Pier Giuseppe Sessa, Haitham Bou Ammar, and Ilija Bogunovic. Group robust preference optimization in reward-free rlhf. *arXiv preprint arXiv:2405.20304*, 2024.
- Zhihong Shao, Peiyi Wang, Qihao Zhu, Runxin Xu, Junxiao Song, Xiao Bi, Haowei Zhang, Mingchuan Zhang, YK Li, Y Wu, et al. Deepseekmath: Pushing the limits of mathematical reasoning in open language models. *arXiv preprint arXiv:2402.03300*, 2024.
- Ruizhe Shi, Yifang Chen, Yushi Hu, ALisa Liu, Noah Smith, Hannaneh Hajishirzi, and Simon Du. Decoding-time language model alignment with multiple objectives. *arXiv preprint arXiv:2406.18853*, 2024.
- Maurice Sion. On general minimax theorems. 1958.
- Charlie Snell, Jaehoon Lee, Kelvin Xu, and Aviral Kumar. Scaling llm test-time compute optimally can be more effective than scaling model parameters. *arXiv preprint arXiv:2408.03314*, 2024.
- Seongho Son, William Bankes, Sayak Ray Chowdhury, Brooks Paige, and Ilija Bogunovic. Right now, wrong then: Non-stationary direct preference optimization under preference drift. *arXiv preprint arXiv:2407.18676*, 2024.
- Taylor Sorensen, Liwei Jiang, Jena D Hwang, Sydney Levine, Valentina Pyatkin, Peter West, Nouha Dziri, Ximing Lu, Kavel Rao, Chandra Bhagavatula, et al. Value kaleidoscope: Engaging ai with pluralistic human values, rights, and duties. In *Proceedings of the AAAI Conference on Artificial Intelligence*, volume 38, pages 19937–19947, 2024a.
- Taylor Sorensen, Jared Moore, Jillian Fisher, Mitchell Gordon, Niloofar Mireshghallah, Christopher Michael Rytting, Andre Ye, Liwei Jiang, Ximing Lu, Nouha Dziri, et al. A roadmap to pluralistic alignment. *arXiv preprint arXiv:2402.05070*, 2024b.
- Nisan Stiennon, Long Ouyang, Jeffrey Wu, Daniel Ziegler, Ryan Lowe, Chelsea Voss, Alec Radford, Dario Amodei, and Paul F Christiano. Learning to summarize with human feedback. *Advances in Neural Information Processing Systems*, 33:3008–3021, 2020.
- Hugo Touvron, Louis Martin, Kevin Stone, Peter Albert, Amjad Almahairi, Yasmine Babaei, Nikolay Bashlykov, Soumya Batra, Prajjwal Bhargava, Shruti Bhosale, et al. Llama 2: Open foundation and fine-tuned chat models. *arXiv preprint arXiv:2307.09288*, 2023.
- J v. Neumann. Zur theorie der gesellschaftsspiele. *Mathematische annalen*, 100(1):295–320, 1928.
- Peter Vamplew, Richard Dazeley, Cameron Foale, Sally Firmin, and Jane Mummary. Human-aligned artificial intelligence is a multiobjective problem. *Ethics and information technology*, 20:27–40, 2018.
- Danqing Wang, Kevin Yang, Hanlin Zhu, Xiaomeng Yang, Andrew Cohen, Lei Li, and Yuandong Tian. Learning personalized story evaluation. *arXiv preprint arXiv:2310.03304*, 2023.
- Haoxiang Wang, Yong Lin, Wei Xiong, Rui Yang, Shizhe Diao, Shuang Qiu, Han Zhao, and Tong Zhang. Arithmetic control of llms for diverse user preferences: Directional preference alignment with multi-objective rewards. *arXiv preprint arXiv:2402.18571*, 2024a.
- Kaiwen Wang, Rahul Kidambi, Ryan Sullivan, Alekh Agarwal, Christoph Dann, Andrea Michi, Marco Gelmi, Yunxuan Li, Raghav Gupta, Avinava Dubey, et al. Conditioned language policy: A general framework for steerable multi-objective finetuning. *arXiv preprint arXiv:2407.15762*, 2024b.
- Mitchell Wortsman, Gabriel Ilharco, Samir Ya Gadre, Rebecca Roelofs, Raphael Gontijo-Lopes, Ari S Morcos, Hongseok Namkoong, Ali Farhadi, Yair Carmon, Simon Kornblith, et al. Model soups: averaging weights of multiple fine-tuned models improves accuracy without increasing inference time. In *International conference on machine learning*, pages 23965–23998. PMLR, 2022.
- Yue Wu, Zhiqing Sun, Huizhuo Yuan, Kaixuan Ji, Yiming Yang, and Quanquan Gu. Self-play preference optimization for language model alignment. *arXiv preprint arXiv:2405.00675*, 2024.
- Zeqi Wu, Yushi Hu, Weijia Shi, Nouha Dziri, Alane Suhr, Prithviraj Ammanabrolu, Noah A Smith, Mari Ostendorf, and Hannaneh Hajishirzi. Fine-grained human feedback gives better rewards for language model training. *Advances in Neural Information Processing Systems*, 36:59008–59033, 2023.
- Tengyu Xu, Eryk Helenowski, Karthik Abinav Sankararaman, Di Jin, Kaiyan Peng, Eric Han, Shaoliang Nie, Chen Zhu, Hejia Zhang, Wenxuan Zhou, et al. The perfect blend: Redefining rlhf with mixture of judges. *arXiv preprint arXiv:2409.20370*, 2024a.
- Zhangchen Xu, Fengqing Jiang, Luyao Niu, Jinyuan Jia, Bill Yuchen Lin, and Radha Poovendran. Safedecoding: Defending against jailbreak attacks via safety-aware decoding. *arXiv preprint arXiv:2402.08983*, 2024b.
- Kailai Yang, Zhiwei Liu, Qianqian Xie, Tianlin Zhang, Nirui Song, Jimin Huang, Ziyang Kuang, and Sophia Ananiadou. Metaaligner: Conditional weak-to-strong correction for generalizable multi-objective alignment of language models. *arXiv preprint arXiv:2403.17141*, 2024.

- Kevin Yang and Dan Klein. Fudge: Controlled text generation with future discriminators. *arXiv preprint arXiv:2104.05218*, 2021.
- Xudong Yu, Chenjia Bai, Haoran He, Changhong Wang, and Xuelong Li. Regularized conditional diffusion model for multi-task preference alignment. *arXiv preprint arXiv:2404.04920*, 2024.
- Siyan Zhao, John Dang, and Aditya Grover. Group preference optimization: Few-shot alignment of large language models. *arXiv preprint arXiv:2310.11523*, 2023.
- Stephen Zhao, Rob Breckelmanns, Alireza Makhzani, and Roger Grosse. Probabilistic inference in language models via twisted sequential monte carlo. *arXiv preprint arXiv:2404.17546*, 2024a.
- Xuandong Zhao, Xianjun Yang, Tianyu Pang, Chao Du, Lei Li, Yu-Xiang Wang, and William Yang Wang. Weak-to-strong jailbreaking on large language models. *arXiv preprint arXiv:2401.17256*, 2024b.
- Yifan Zhong, Chengdong Ma, Xiaoyuan Zhang, Ziran Yang, Haojun Chen, Qingfu Zhang, Siyuan Qi, and Yaodong Yang. Panacea: Pareto alignment via preference adaptation for llms. *arXiv preprint arXiv:2402.02030*, 2024.
- Zhanhui Zhou, Jie Liu, Chao Yang, Jing Shao, Yu Liu, Xiangyu Yue, Wanli Ouyang, and Yu Qiao. Beyond one-preference-for-all: Multi-objective direct preference optimization. *arXiv preprint arXiv:2310.03708*, 2023.
- Zhanhui Zhou, Zhixuan Liu, Jie Liu, Zhichen Dong, Chao Yang, and Yu Qiao. Weak-to-strong search: Align large language models via searching over small language models. *arXiv preprint arXiv:2405.19262*, 2024.
- Baiting Zhu, Meihua Dang, and Aditya Grover. Scaling pareto-efficient decision making via offline multi-objective rl. *arXiv preprint arXiv:2305.00567*, 2023.
- Martin Zinkevich, Michael Johanson, Michael Bowling, and Carmelo Piccione. Regret minimization in games with incomplete information. *Advances in neural information processing systems*, 20, 2007.

Appendix Contents

In Appendix A, we provide the proofs to the propositions and detailed derivation of simplifying the optimization objective introduced in the paper. We also analyze the characteristics of the weights computed by RMOD in Appendix B. We provide the skipped details of the experimental setup and additional experiments in Appendix C. In Appendix D, we introduce a no-regret learning algorithm for optimizing the robust alignment objective. We further discuss the works relevant to our approach in Appendix E.

A Proofs of RMOD Optimization

In this section, we detail the proofs of the propositions and the objective for optimal weights in Equation (7) outlined in Section 2.2.

A.1 Non-robust Decoding Objective

Proposition A.1. *Given the value functions V_g for each objective $g \in \mathcal{G}$, the solution to the inner maximization problem in Equation (5) is unique for any given weights w and trade-off parameter λ , and can be expressed as*

$$\pi(z|[x, y^t]; w) = \frac{\pi_{\text{ref}}(z|[x, y^t]) \exp\left(\lambda \sum_{g=1}^G w_g V_g(x, y^t; z)\right)}{Z(x, y^t, w)}, \quad (6)$$

where, $Z(x, y^t, w)$ is a normalization constant.

Proof. We reiterate the inner maximization problem detailed in Equation (4) in terms of the weighted value function:

$$\max_{\pi} \lambda \sum_{g=1}^G w_g V_g(x, y^t; \pi) - D_{\text{KL}}(\pi \parallel \pi_{\text{ref}}).$$

Here, the KL divergence $D_{\text{KL}}(\pi \parallel \pi_{\text{ref}}) = \mathbb{E}_{z \sim \pi(z|[x, y^t])} [\log(\pi(z|[x, y^t]) / \pi_{\text{ref}}(z|[x, y^t]))]$ regularizes π to stay close to π_{ref} , preventing reward over-optimization. The coefficient λ governs the degree of regularization. The proof follows a similar strategy to that of Mudgal et al. [2023, Theorem-2.1].

We note that the maximization objective can be rewritten as

$$\begin{aligned} \lambda \sum_{g=1}^G w_g V_g(x, y^t; \pi) - D_{\text{KL}}(\pi \parallel \pi_{\text{ref}}) &= \sum_{z \in \mathcal{Z}} \pi(z|[x, y^t]) \left[\lambda \sum_{g=1}^G w_g V_g(x, y^t; z) + \log \left(\frac{\pi_{\text{ref}}(z|[x, y^t])}{\pi(z|[x, y^t])} \right) \right] \\ &= \sum_{z \in \mathcal{Z}} \pi(z|[x, y^t]) \log \left(\frac{\pi_{\text{ref}}(z|[x, y^t]) e^{\lambda \sum_{g=1}^G w_g V_g(x, y^t; z)}}{\pi(z|[x, y^t])} \right). \end{aligned}$$

We define

$$q_{\lambda}(z|[x, y^t]) := \frac{\pi_{\text{ref}}(z|[x, y^t]) e^{\lambda \sum_{g=1}^G w_g V_g(x, y^t; z)}}{Z(x, y^t, w)} \quad (13)$$

where $Z(x, y^t, w) = \sum_{z \in \mathcal{Z}} \pi_{\text{ref}}(z|[x, y^t]) e^{\lambda \sum_{g=1}^G w_g V_g(x, y^t; z)}$. Rewriting the objective based on $q_{\lambda}(\cdot|[x, y^t])$, we obtain

$$\lambda \sum_{g=1}^G w_g V_g(x, y^t; \pi) - D_{\text{KL}}(\pi \parallel \pi_{\text{ref}}) = -D_{\text{KL}}(\pi \parallel q_{\lambda}(\cdot|[x, y^t])) + \log Z(x, y^t, w). \quad (14)$$

We note that this objective in Equation (14) is strongly concave in π , and the unique maximizer is given by

$$\pi(\cdot|[x, y^t]; w) = q_{\lambda}(\cdot|[x, y^t]). \quad (15)$$

□

A.2 Proof of Proposition 3.2

Proposition A.2. *The solution w^* to the convex optimization problem in Equation (7) and $\pi^* = \pi(\cdot; w^*)$ in Equation (6) constitute a Nash Equilibrium for the max-min game in Equation (4).*

Proof. We first restate Equation (7), where

$$w^* = \arg \min_{w \in \Delta^{G-1}} \log \mathbb{E}_{z \sim \pi_{\text{ref}}(\cdot | [x, y^t])} [f(z; x, y^t, w)], \quad (16)$$

$$f(z; x, y^t, w) = \exp \left(\sum_{g=1}^G \lambda w_g V_g(x, y^t; z) \right). \quad (17)$$

We note that Equation (17) is the result of substituting the policy π in Equation (5) with *best-response policy*, $\pi(\cdot; w)$ (see Equation (6)), for given weights w . By computing w^* in Equation (17), we obtain the best-response weights against $\pi(\cdot; w)$. Representing the weight vector and the policy as players in the game, both w^* and $\pi(\cdot; w^*)$ are best responses to each other. This means that the weights and the policy are in a Nash Equilibrium. \square

A.3 Simplification of RMOD optimization problem

The concave-convex objective in Equation (4) in terms of π and w allows the interchange of minimum and maximum operators. We re-write Equation (4) as

$$\min_{w \in \Delta^{G-1}} \max_{\pi} \lambda \sum_{g=1}^G w_g V_g(x, y^t; \pi) - D_{\text{KL}}(\pi \| \pi_{\text{ref}}). \quad (18)$$

Moreover, we characterize the optimal policy for the inner maximization problem for any given weights w and trade-off parameter λ in Proposition 3.1 as

$$\pi(z | [x, y^t]; w) = \frac{\pi_{\text{ref}}(z | [x, y^t]) \exp \left(\lambda \sum_{g=1}^G w_g V_g(x, y^t; z) \right)}{Z(x, y^t, w)}, \quad (19)$$

where $Z(x, y^t, w) = \sum_{z \in \mathcal{Z}} \pi_{\text{ref}}(z | [x, y^t]) \exp \left(\lambda \sum_{g=1}^G w_g V_g(x, y^t; z) \right)$ is a normalization constant. Here, the weight-conditioned policy, $\pi(\cdot; w)$, is the *best-response policy* to weights w . Plugging Equation (19) back to Equation (18), and minimizing in terms of w , we obtain

$$\begin{aligned} & \min_{w \in \Delta^{G-1}} \lambda \sum_{g=1}^G w_g \left(\sum_{z \in \mathcal{Z}} \pi(z | [x, y^t]; w) V_g(x, y^t; z) \right) \\ & - \sum_{z \in \mathcal{Z}} \pi(z | [x, y^t]; w) \log \left(\frac{\pi_{\text{ref}}(z | [x, y^t]) \exp \left(\lambda \sum_{g=1}^G w_g V_g(x, y^t; z) \right)}{\pi_{\text{ref}}(z | [x, y^t]) Z(x, y^t, w)} \right). \end{aligned} \quad (20)$$

Since $\pi_{\text{ref}}(z | [x, y^t])$ cancels out in the log term, we simplify Equation (20):

$$\min_{w \in \Delta^{G-1}} \lambda \sum_{g=1}^G w_g \left(\sum_{z \in \mathcal{Z}} \pi(z | [x, y^t]; w) V_g(x, y^t; z) \right) - \quad (21)$$

$$\begin{aligned} & \sum_{z \in \mathcal{Z}} \pi(z | [x, y^t]; w) \left(\sum_{g=1}^G \lambda w_g V_g(x, y^t; z) - \log(Z(x, y^t, w)) \right) \\ & = \min_{w \in \Delta^{G-1}} \lambda \sum_{g=1}^G w_g \left(\sum_{z \in \mathcal{Z}} \pi(z | [x, y^t]; w) V_g(x, y^t; z) \right) - \quad (22) \end{aligned}$$

$$\begin{aligned} & \lambda \sum_{g=1}^G w_g \left(\sum_{z \in \mathcal{Z}} \pi(z | [x, y^t]; w) V_g(x, y^t; z) \right) + \sum_{z \in \mathcal{Z}} \pi(z | [x, y^t]; w) \log(Z(x, y^t, w)) \\ & = \min_{w \in \Delta^{G-1}} \log(Z(x, y^t, w)). \end{aligned} \quad (23)$$

If we denote the solution of Equation (23) as w^* , then w^* is also the solution of $\min_{w \in \Delta^{G-1}} Z(x, y^t, w)$ due to the monotonicity of log. From the definition of $Z(x, y^t, w)$, this optimization is written as follows:

$$\min_{w \in \Delta^{G-1}} \sum_{z \in \mathcal{Z}} \pi_{\text{ref}}(z | [x, y^t]) \exp \left(\sum_{g=1}^G \lambda w_g \cdot V_g(x, y^t; z) \right). \quad (24)$$

A.4 Gradient Descent on $\log w$

In Section 4, Algorithm 2 implements gradient descent update w.r.t. the logits of w . Suppose $e^{l_g} \propto w_g$. The update for logits l_g is

$$l_{g,i+1} := l_{g,i} - \eta \nabla_{l_g} \sum_{z \in \mathcal{Z}} \pi_{\text{ref}}(z | [x, y^t]) \exp \left(\sum_{g=1}^{|G|} \lambda e^{l_g} V_g(x, y^t; z) \right) |_{l_g=l_{g,i}} \quad (25)$$

$$= l_{g,i} - \eta \sum_{z \in \mathcal{Z}} \pi_{\text{ref}}(z | [x, y^t]) \exp \left(\sum_{g=1}^{|G|} \lambda e^{l_{g,i}} V_g(x, y^t; z) \right) \nabla_{l_g} \sum_{g=1}^{|G|} \lambda e^{l_g} V_g(x, y^t; z) |_{l_g=l_{g,i}}, \quad (26)$$

$$= l_{g,i} - \eta \sum_{z \in \mathcal{Z}} \pi_{\text{ref}}(z | [x, y^t]) \exp \left(\sum_{g=1}^{|G|} \lambda e^{l_{g,i}} V_g(x, y^t; z) \right) \lambda e^{l_{g,i}} V_g(x, y^t; z). \quad (27)$$

Therefore, the logarithm of weight is updated as

$$\log w_{g,i+1} := \log w_{g,i} - \eta \sum_{z \in \mathcal{Z}} \pi_{\text{ref}}(z | [x, y^t]) \exp \left(\sum_{g=1}^{|G|} \lambda w_{g,i} V_g(x, y^t; z) \right) \lambda w_{g,i} V_g(x, y^t; z). \quad (28)$$

And thus the weight is updated by computing

$$w_{g,i+1} := w_{g,i} \cdot \exp \left[- \eta \sum_{z \in \mathcal{Z}} \pi_{\text{ref}}(z | [x, y^t]) \exp \left(\sum_{g=1}^{|G|} \lambda w_{g,i} V_g(x, y^t; z) \right) \lambda w_{g,i} V_g(x, y^t; z) \right]. \quad (29)$$

B Analysis of Weights Computed by RMOD

The optimal weight w^* is obtained by solving the constrained optimization Equation (7), which is a convex optimization problem. The log-sum-exp function is convex, and the feasible set is a simplex. This optimization may not have an analytic solution, but we can obtain some insight by writing its Lagrangian $L(w, \alpha, \beta)$ where $\alpha \in \mathbb{R}$ and $\beta \in (\mathbb{R}^+)^G$ are Lagrange multipliers. The Lagrangian of the problem is written as follows:

$$L(w, \alpha, \beta) = \log \mathbb{E}_{z \sim \pi_{\text{ref}}} \left[\exp \left(\lambda \sum_{g=1}^G w_g V_g(x, y^t; z) \right) \right] - \alpha \left(\sum_g w_g - 1 \right) - \sum_g \beta_g w_g. \quad (30)$$

Each weight component w_g may or may not be zero and as such the optimality condition for each case can be derived separately.

Non-zero weight w_g . For the index g with $w_g > 0$, we have $\beta_g = 0$ from the complementary slackness. Then, we can set the partial derivative of L to be zero. Note, $\mathbb{E}_{z \sim \pi} [V_g(x, y^t; z)] = V_g(x, y^t; \pi)$.

$$\frac{\partial L}{\partial w_g} = \frac{\mathbb{E}_{z \sim \pi_{\text{ref}}} \left[\exp \left(\lambda \sum_{g=1}^G w_g V_g(x, y^t; z) \right) V_g(x, y^t; z) \right]}{\mathbb{E}_{z \sim \pi_{\text{ref}}} \left[\exp \left(\lambda \sum_{g=1}^G w_g V_g(x, y^t; z) \right) \right]} \cdot \lambda - \alpha = 0. \quad (31)$$

The denominator is the normalization constant $Z(x, y^t, w)$ of $\pi(z|x, y^t)$, defined in Equation (6). Then, the optimality condition says that the g -th value function is constant.

$$\mathbb{E}_{z \sim \pi_{\text{ref}}} \left[\frac{1}{Z(x, y^t, w)} \exp \left(\lambda \sum_{g=1}^G w_g V_g(x, y^t; z) \right) V_g(x, y^t; z) \right] \quad (32)$$

$$= \mathbb{E}_{z \sim \pi} [V_g(x, y^t; z)] = V_g(x, y^t; \pi) = \frac{\alpha}{\lambda} \quad (33)$$

Therefore, the weights optimized for group robustness result in identical values of π across all g 's that are $w_g > 0$.

Zero weight w_g . Similarly, we can derive the optimality condition for w_g that is zero. In such cases, we have $\beta_g > 0$, leading to a different stationary condition as follows:

$$\frac{\partial L}{\partial w_g} = \frac{\mathbb{E}_{z \sim \pi_{\text{ref}}} \left[\exp \left(\lambda \sum_{g=1}^G w_g V_g(x, y^t; z) \right) V_g(x, y^t; z) \right]}{\mathbb{E}_{z \sim \pi_{\text{ref}}} \left[\exp \left(\lambda \sum_{g=1}^G w_g V_g(x, y^t; z) \right) \right]} \cdot \lambda - \alpha - \beta_g = 0. \quad (34)$$

Arranging the above condition results in the following:

$$\mathbb{E}_{z \sim \pi} [V_g(x, y^t; z)] = V_g(x, y^t; \pi) = \frac{\alpha + \beta_g}{\lambda}. \quad (35)$$

Since $\beta_g > 0$, the corresponding value function is larger than α/λ , which is the value function with non-zero weight. Roughly speaking, $w_g = 0$ indicates that the group’s expected value is larger than the expected value of worst-case groups.

C Further Experimental Details

C.1 Experimental Setup

The Helpfulness-Harmlessness dataset. The task of LLM in this dataset is to provide as helpful answer as possible, while not generating any content in the response that is potentially harmful. This is tested by some prompts asking for generic information like desining a workout routine, while some others are asking for insult examples and private information. We use `gpt2-large-helpful-reward` model and `gpt2-large-harmless-reward` model to evaluate the helpfulness and harmlessness reward of the LLM responses respectively. We train a value function whose weights are initialized from `gpt2-large-harmless-reward` model, while we substitute the last layer with a fully connected layer with 2 outputs. We generate up to 256 tokens of response using `gemma-2-2b-it` as the reference model for each training prompt, and use the same length for generating test responses.

The UltraFeedback Dataset. We evaluate the LLM’s general ability to provide appropriate answers by using the prompts in the UltraFeedback dataset, which ranges from code writing to providing an analogy. For the UltraFeedback dataset, we use 5 rewards for the value function training and evaluation: CONCISENESS, INSTRUCTION FOLLOWING, TRUTHFULNESS, HONESTY and HELPFULNESS. We multiply -1 to `HELPSTEER-VERBOSITY` from ARMORM to compute the CONCISENESS reward. Once the rewards to the responses generated from π_{ref} are obtained, we also apply normalization to each reward to prevent the scale difference from affecting the experiment. For the UltraFeedback dataset, we train a value function initialized from `gpt2-large-harmless-reward_model` for each reward and use 5 value functions together for decoding. For evaluation, we report the rewards from ARMORM with normalization using the same mean and standard deviation computed in the training dataset. Up to 128 tokens were generated using `gemma-2-2b-it` for each response in the training set, while we exclude prompts longer than 200 tokens to make sure the sequence length is within the limit of GPT2-based value functions.

The ValuePrism Dataset. Using the ValuePrism dataset, we set up a multi-value commentary generation task, where an LLM is asked to generate a response that aligns with multiple human values. An LLM is prompted to generate a single-sentence comment on a situation in the `situation` field of the ValuePrism dataset. The prompt is formatted as “Please comment on the following situation in a single sentence: {situation}.” The reward in this task is defined as the probability of support, which quantifies how much the response supports a certain VRD (value, right, and duty) given in ValuePrism. The support probability is computed by `kaleido-xl` model using `get_valence()` function. We choose the top 10 most frequently occurring VRDs (value, right, and duty) in ValuePrism, namely, Autonomy, Right to life, Justice, Compassion, Well-being, Duty of care, Respect, Safety, Right to property, and Responsibility, in the order of decreasing frequency. When varying the number of rewards, we start with the most frequent rewards and then gradually incorporate the less frequent rewards. For example, for an experiment with four rewards, an LLM aligns towards Autonomy, Right to life, Justice, and Compassion.

Fine-tuning Baselines. The DPO baselines for the HH dataset are trained using a preference dataset created from the same dataset used to learn the value functions in HH. For each prompt in the dataset, four responses are generated; each of these samples is then evaluated by the two reward functions. To create the preference dataset, pairs of responses are combined using the relevant reward values to determine the preference labels within the dataset. For the Group Relative Policy Optimization (GRPO) Shao et al. [2024] baseline, 8 responses are sampled for each prompt at each training step. GRPO was chosen because of its strong performance and light computational requirement relative to traditional approaches, e.g. PPO.

Reward Soup and Multi-Objective Decoding Baseline. The Reward Soup (RS) Rame et al. [2024] and Multi-Objective Decoding (MOD) Shi et al. [2024] baselines combine multiple fine-tuned models to create a multi-objective

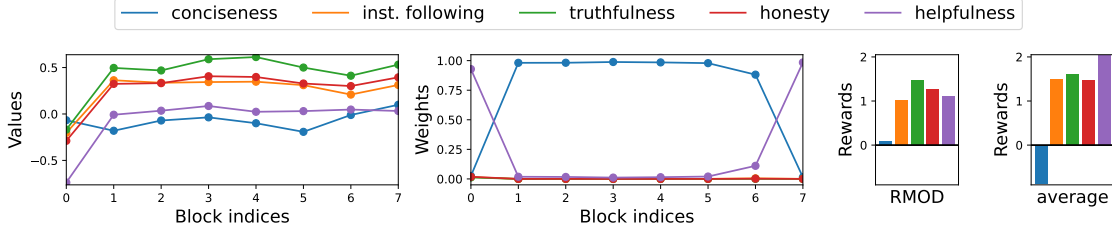


Figure 7: Analysis of RMOD’s weight and value predictions in the generation of a response presented in Appendix C.4. During most of the decoding process, RMOD allocates most of the weight on the CONCISENESS value, which results in a significant improvement when compared to UNIFORM decoding. It also allocates weights on the HELPFULNESS reward in the beginning and the end of the generation, preventing the response from becoming only a short sequence without fulfilling the request from the prompt.

aligned LLM. We define $\pi_g(y|x; \phi_g)$ as the policy fine-tuned on the reward model r_g with parameters ϕ_g . Samples are generated from Reward Soup as:

$$y \sim \pi(y|x; \sum_{g \in G} w_g \phi_g) \quad (36)$$

where $\sum_{g \in G} w_g = 1$. Multi-Objective Decoding combines the policies π_g at inference time, and samples each new token y_t from the weighted sum of the models logits, this can alternatively be written as:

$$y_t \sim \prod_{g \in G} \pi(y_t|y^{t-1}, x; \phi_g)^{w_g}. \quad (37)$$

Both approaches require access to π_g , models fine-tuned on a single reward model r_g . In our experiments, we use policies trained with GRPO for each reward.

Compute. Experiments are run on a A100 80GB GPU.

C.2 Comparison with Best-of- K

As noted in the main text, setting the block size to the length of the entire sequence in blockwise decoding is equivalent to Best-of- K rejection sampling. In order to investigate the effectiveness of blockwise RMOD, we compare the worst-case rewards of both methods along the change of K . We use 1024 prompts from the HH dataset to generate the responses, while Best-of- K methods generate K responses with $B = 256$ tokens at once while blockwise decoding methods use $B = 16$. As shown in Figure 8, blockwise decoding methods including RMOD with $B = 16$ achieve much higher worst-case reward at lower values of K . At $K = 4$, blockwise decoding methods already achieve rewards higher than Best-of-16. Considering that value functions can have much smaller parameter size than the policy and that value function evaluations happen every B tokens, Figure 8 shows that blockwise decoding methods are better than Best-of- K methods in both terms of performance and compute efficiency.

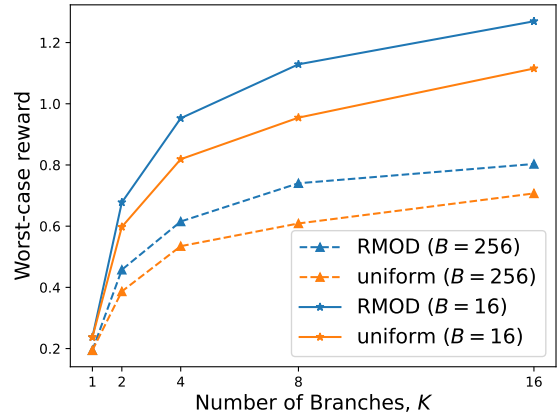


Figure 8: Comparison between blockwise decoding methods and Best-of- K rejection sampling in the **HH** dataset. Blockwise decoding methods ($B = 16$) significantly outperform Best-of- K methods ($B = 256$) already at $K = 4$.

C.3 Latency Comparison

In Section 4 we introduce a variety of approximations to Algorithm 1 to produce the practical algorithm shown in Algorithm 2. We now compare the computational efficiency of Algorithm 2 with the Controlled Decoding algorithm from Mudgal et al. [2023]. We run decoding across 100 prompts from the Ultrafeedback dataset, and record the time to produce B tokens, where B is the block size, and the total run time to decode the entire response. We observe no statistically significant difference in the run times as shown in Figure 9. Whilst RMOD solves an optimization

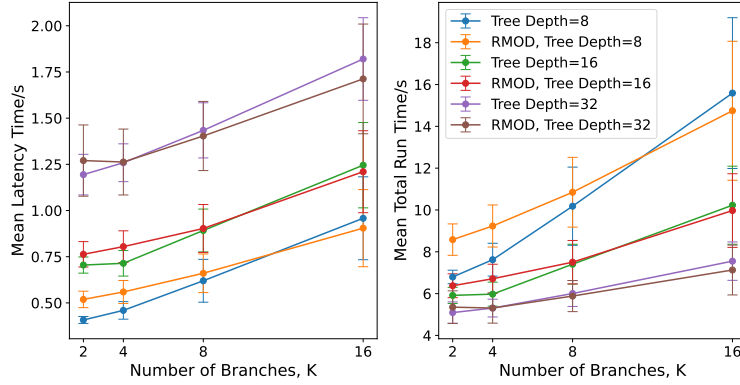


Figure 9: A comparison of the decoding timings of RMOD and UNIFORM; RMOD has the same latency and total run time as the Controlled Decoding [Mudgal et al., 2023] based UNIFORM baseline. [Left] The latency timing is the time in seconds to produce B tokens that can be immediately returned to the user, where B is the tree depth. [Right] The total run time is the time in seconds taken to return the entire response to the user. All experiments are run on 100 prompts from the Ultrafeedback dataset in batches of 2 on a single A100 80GB GPU.

problem during decoding, the problem is low dimensional and solving it is thus far quicker than the main computational bottleneck - forward passes through the LLM.

C.4 Investigating the RMOD generation

To qualitatively investigate the performance of RMOD, we present and compare the actual responses generated by RMOD and UNIFORM decoding. We also provide the same figure as Figure 5 in Figure 7 for the presented response. Here we present the result of using $B = 16$, $K = 16$ and generating up to 128 tokens for the response for a prompt sampled from the UltraFeedback dataset. We give the following prompt for both methods to generate a response:

Can you describe a process using the following phrase as a template:
 "[Action A] is to [Object B] as [Action C] is to [Object D]"?
 Please provide an example using the phrase
 "Digestion is to food as coding is to software development".

To the prompt above, UNIFORM decoding generates the following response:

Here's an example using your template:

```

**"Digestion is to food as coding is to software development."**

**Explanation:**

* **Action A:** Digestion
* **Object B:** Food

* **Action C:** Coding
* **Object D:** Software development

**Description:**

Digestion is the process of breaking down food into absorbable nutrients.
Coding is the process of designing instructions (algorithms)
to create software products.

**Thus, digestion is the action of preparing a given substance (food)
for ingestion and utilization, just as coding prepares the conceptual

```

framework of specific software creations.**

The response generated by UNIFORM is using more tokens to convey the information in detail, which resulted in losing conciseness reward. On the other hand, RMOD generates a response that is much more *concise*:

Yes, here's an example using your template:

****Digestion is to food as coding is to software development.****

* ****Digestion**** is the process of breaking down food.
 * ****Food**** is the ingredient being processed.
 * ****Coding**** is the process of writing programs.
 * ****Software development**** is the bigger field where programs are created.

Let me know if you'd like to try another example!

The response generated by RMOD clearly shows that fewer tokens are used while containing only the most necessary ones to provide relevant answer to the prompt. As shown in Figure 7, the response generated by RMOD above is the result of putting significant weight on the CONCISENESS objective during the generation. This leads to improved CONCISENESS reward compared to UNIFORM, and the qualitative difference between the responses is shown by the token length and the organization of the response. This example further supports the effectiveness of RMOD, providing evidence that our method successfully balances the alignment objectives and is able to output qualitatively distinguishable responses.

D Alternative Methods for Max-Min Game Solving

In this section, we discuss some of the classical strategies for solving max-min games and compare them with our method detailed in Section 3. We define the the payoff (utility function) w.r.t. value function $V_g(x, y^t; z)$, weights \mathbf{w} and policy π as follows:

$$U(\pi, \mathbf{w}) = \lambda \left[\sum_{g=1}^{|\mathcal{G}|} w_g \sum_{z \in \mathcal{Z}} \pi(z | [x, y^t]) V_g(x, y^t; z) \right] - \sum_{z \in \mathcal{Z}} \pi(z | [x, y^t]) \log \left(\frac{\pi(z | [x, y^t])}{\pi_{\text{ref}}(z | [x, y^t])} \right). \quad (38)$$

Moreover, for a given token z sampled from π at $[x, y^t]$, the payoff is as follows:

$$U(z, \mathbf{w}) = \lambda \left[\sum_{g=1}^{|\mathcal{G}|} w_g \pi(z | [x, y^t]) V_g(x, y^t; z) \right] - \log \left(\frac{\pi(z | [x, y^t])}{\pi_{\text{ref}}(z | [x, y^t])} \right). \quad (39)$$

We can equivalently define the bandit loss of \mathbf{w} from the payoff definition. Consequently, we can apply various learning algorithms for solving this max-min game which we outline next.

D.1 Solving Robust Multi-Objective Decoding with No-Regret Weights Learning

Regret Minimization (i.e., No-Regret Learning) has been extensively studied to solve zero-sum max-min games [Zinkevich et al., 2007, Lanctot et al., 2009, Chhablani et al., 2023, Bailey and Piliouras, 2018]. Typically, convergence to the Nash Equilibrium requires policy averaging and no-regret update in a self-play manner. We discuss such a suitable no-regret learning procedure, *Hedge* Update [Freund and Schapire, 1997], in the context of our work below.

We apply *Hedge* update for solving Equation (4) on group weights and a *best-response* update on the policy, iteratively. We call such iterative process *Hedge-BR*. Although it is not typical self-play no-regret learning, it is guaranteed to converge to the Nash Equilibrium [Johanson et al., 2012, McAleer et al., 2022].

We introduce the algorithm as follows. We initialize π_0 with reference policy. At iteration i , for a given policy π^i , we update the group weights following *Hedge* [Freund and Schapire, 1997] as follows:

$$w_g^{i+1} \propto w_g^i \cdot \exp \left\{ -\eta \mathbb{E}_{\pi^i(z|[x, y^t])} [V_g(x, y^t; z)] + D_{\text{KL}}(\pi \parallel \pi_{\text{ref}}) \right\}. \quad (40)$$

Given the group weights at iteration $i + 1$, the policy is updated with the *best-response* update:

$$\pi^{i+1}(z | [x, y^t]) = \arg \max_{\pi} \sum_{g=1}^{|\mathcal{G}|} \lambda w_g^i V_g(x, y^t; \pi) - D_{\text{KL}}(\pi \parallel \pi_{\text{ref}}). \quad (41)$$

For simplicity, we abbreviate

$$f(z; x, y^t, w) = \exp \left(\sum_{g=1}^{|\mathcal{G}|} \lambda w_g^i V_g(x, y^t; z) \right). \quad (42)$$

Then, Equation (41) has the following closed-form solution from Proposition 3.1:

$$\frac{\pi^{i+1}(z \mid [x, y^t])}{\pi_{\text{ref}}(z \mid [x, y^t])} \propto f(z; x, y^t, w). \quad (43)$$

We denote the joint average strategy as the average group weights $\bar{w}_g = \sum_{i=0}^I w_g^i / (I + 1)$ and its corresponding best response from Equation (43) with $w = \bar{w}$. Next, we demonstrate that this iterative process leads to the convergence of the joint average strategy to the Nash equilibrium. According to Proposition 3 [McAleer et al., 2022] and Theorem 3 [Johanson et al., 2012], after I iterations of group weights w update with *Hedge* (see Equation (40)), and policy π update with *best-response* (see Equation (43)), alternately, the joint average strategy is an ϵ -Nash Equilibrium, where $\epsilon = \mathcal{O}(1/\sqrt{I})$.

Reduction to Weights Only Update. According to the policy update rule in Equation (43):

$$\pi^i(z \mid [x, y^t]; w) = \frac{\pi_{\text{ref}}(z \mid [x, y^t]) \exp \left(\sum_{g=1}^{|\mathcal{G}|} \lambda w_g^i \cdot V_g(x, y^t; z) \right)}{Z(x, y^t, w^i)}, \quad (44)$$

where the normalization constant is

$$Z(x, y^t, w^i) = \sum_{z \in \mathcal{Z}} \pi_{\text{ref}}(z \mid [x, y^t]) \exp \left(\sum_{g=1}^{|\mathcal{G}|} \lambda w_g^i \cdot V_g(x, y^t; z) \right). \quad (45)$$

We substitute this optimal policy back into group weight Hedge update in Equation (40) to obtain

$$\begin{aligned} w_g^{i+1} \propto w_g^i \cdot \exp & \left[-\eta \left(\sum_{z \in \mathcal{Z}} \pi(z \mid [x, y^t]; w) V_g(x, y^t; z) \right) \right. \\ & \left. - \sum_{z \in \mathcal{Z}} \pi(z \mid [x, y^t]; w^i) \log \left(\frac{\pi_{\text{ref}}(z \mid [x, y^t]) \exp \left(\sum_{g=1}^{|\mathcal{G}|} \lambda w_g^i \cdot V_g(x, y^t; z) \right)}{\pi_{\text{ref}}(z \mid [x, y^t]) Z(x, y^t, w^i)} \right) \right]. \end{aligned} \quad (46)$$

Since the latter term inside the exponential is independent of g , it can be removed and the weight update becomes:

$$w_g^{i+1} \propto w_g^i \cdot \exp \left[-\eta \left(\sum_{z \in \mathcal{Z}} \pi(z \mid [x, y^t]; w) V_g(x, y^t; z) \right) \right] \quad (47)$$

$$\propto \exp \left[-\eta \left(\sum_{z \in \mathcal{Z}} \frac{\pi_{\text{ref}}(z \mid [x, y^t]) \exp \left(\sum_{g=1}^{|\mathcal{G}|} \lambda w_g^i \cdot V_g(x, y^t; z) \right)}{Z(x, y^t, w^i)} V_g(x, y^t; z) \right) \right]. \quad (48)$$

Hence, we can approximate the iterative update process to attain Nash Equilibrium group weights by Equation (48).

D.2 Comparison of No-Regret Learning and Gradient Descent

We compare three different methods, Hedge-BR, gradient-descent (GD) on the logits of group weights, and GD on weights directly which requires projection back to Δ^{G-1} to ensure w remains a probability vector.

The Hedge-BR update is :

$$w_{g,i+1} \propto w_{g,i} \cdot \exp \left[-\eta \left(\sum_{z \in \mathcal{Z}} \frac{\pi_{\text{ref}}(z \mid [x, y^t]) \exp \left(\sum_{g'=1}^{|\mathcal{G}|} \lambda w_{g',i} \cdot V_{g'}(x, y^t; z) \right)}{Z(w^i)} \right) V_g(x, y^t; z) \right]. \quad (49)$$

Meanwhile, as in Equation (12), the update of the weight logits using GD is

$$w_{g,i+1} := w_{g,i} \cdot \exp \left[-\eta \sum_{z \in \mathcal{Z}} \pi_{\text{ref}}(z \mid [x, y^t]) \exp \left(\sum_{g=1}^{|\mathcal{G}|} \lambda w_{g,i} V_g(x, y^t; z) \right) \lambda w_{g,i} V_g(x, y^t; z) \right]. \quad (50)$$

If we apply GD to the weights directly to minimize Z in Equation (23), the weight update is

$$w_{g,i+1} = w_{g,i} - \eta \sum_{z \in \mathcal{Z}} \pi_{\text{ref}}(z \mid [x, y^t]) \exp \left(\sum_{g=1}^{|\mathcal{G}|} \lambda w_{g,i} V_g(x, y^t; z) \right) \lambda V_g(x, y^t; z). \quad (51)$$

The update direction of all the methods in Equation (49), Equation (50) and Equation (51) are similar. GD on logits and Hedge-BR update w by exponential multiplication, while GD on weights updates w by subtraction. The difference between Hedge-BR and GD on logits is only a $w_{g,i}$ factor multiplied to the power of exponent during the exponential update.

E Additional Related Work

Test-time Alignment. Test-time alignment algorithms rely on modifying the output logits of LLMs [Liu et al., 2024a, Zhao et al., 2024b, Huang et al., 2024, Liu et al., 2024b]. Approaches such as Liu et al. [2021], Xu et al. [2024b] combine a pretrained language model with *expert* or *anti-expert* LLMs to modify the token probabilities. Krause et al. [2020] also guide sequence generation by using both desired and undesired attributes to condition the token probabilities via Bayes rule. Utilizing fine-grained human feedback on specific parts of the sequence instead of evaluating the entire response as a whole, Wu et al. [2023] train fine-grained reward models that can give intermediate signals before the generation terminates. Kumar et al. [2022] investigate generation with user-defined constraints by combining the log likelihood of the LLM with arbitrary constraints in an energy function, generating samples in a non-autoregressive manner. A similar approach of using energy functions for specifying constraints is used by Qin et al. [2022] as well. Zhao et al. [2024a] propose a novel contrastive method for learning the twist functions and use them to perform Sequential Monte Carlo (SMC).

Multi-Objective Alignment. Zhu et al. [2023], Basaklar et al. [2022] propose training a policy conditioned on preference weightings across multiple objectives to maximize the expected rewards, which inspired works in multi-objective decoding. Fu et al. [2024] align to multiple objectives at test time using a positive and negative prompt example in context to adjust model logits. Yang et al. [2024] adapts Ji et al. [2024] aligning the policy model to multiple objectives via an external adapter. Badrinath et al. [2024] introduce hybrid objectives to improve the general single objective alignment. Zhong et al. [2024] use Singular Value Decomposition to guide an LLM towards multiple objectives during inference. Xu et al. [2024a] employ a mixture of judge LLMs to help balance multi-objective alignment approaches in practice. Wortsman et al. [2022], Ramé et al. [2024] propose averaging the weights of multiple models fine-tuned with different hyperparameters, improving accuracy and robustness and leading to further investigation in Jang et al. [2023], Rame et al. [2024]. Lin et al. [2024] propose heterogeneously finding model combination ratios of layers for further improvement in performance. Yu et al. [2024], Lee et al. [2024] consider multi-objective alignment in diffusion model architectures.